

WORKSPACE AND JOINT DISPLACEMENT
COMPARISON OF 3R AND 4R ROBOTS

By

ALIREZA BEHBOUD

Bachelor of Science in Mechanical Engineering

Oklahoma State University

Stillwater, Oklahoma

1980

Submitted to the Faculty of the Graduate College
of the Oklahoma State University
in partial fulfillment of the requirements
for the Degree of
MASTER OF SCIENCE
July, 1982

Thesis
1982
B419W
cop. 2



WORKSPACE AND JOINT DISPLACEMENT
COMPARISON OF 3R AND 4R ROBOTS

Thesis Approved:

Abraham H. Inou

Thesis Adviser

Larry Zible

Richard L Lowery

Norman A. Durhan

Dean of Graduate College

ACKNOWLEDGMENTS

I thank my advisor, Dr. A. H. Soni, for his guidance and assistance throughout this study. Also, for his excellent instruction and many interesting discussions in coursework at Oklahoma State University, which provided the background necessary to carry this study through.

I also thank the other members of my advisory committee, Dr. Richard L. Lowery and Dr. Larry D. Zirkle. Dr. Y. C. Tsai provided valuable assistance throughout this study. Thank you.

I want to give special thanks to Ms. Aslaug Haraldsdottir for her valuable assistance in the preparation of the final manuscript for this thesis.

Finally, I thank my parents for their support and encouragement throughout my entire education.

TABLE OF CONTENTS

Chapter	Page
I. INTRODUCTION	1
1.1 Background	1
1.2 Objectives	2
II. A COMPARISON OF THE WORKSPACES OF 3R AND 4R ROBOTS	3
2.1 Definition of the Workspace of a Robot Hand	3
2.2 Mathematical Concepts for Workspace Analysis	3
2.3 Basic Considerations in Choosing the 'Right Robot'	6
2.4 The Type of Robot under Consideration	8
2.5 Method of Analysis and Results	10
III. JOINT DISPLACEMENT ANALYSIS	21
3.1 Introduction	21
3.2 A Comparison of Joint Displacements of the 'Popular' 3R Robot and General 4R Robots	22
3.3 The Iterative Velocity Method	26
3.4 Examples of Joint Displacement Analysis	31
IV. THE EFFECT OF SPACE CONSTRAINTS ON THE WORKSPACE OF 3R AND 4R ROBOTS	35
4.1 Introduction	35
4.2 Workspace Analysis in the Presence of Space Constraints	35
V. SUMMARY AND RECOMMENDATIONS	53
5.1 Summary	53
5.2 Recommendations	54
REFERENCES	56
APPENDIXES	57
APPENDIX A - LISTING OF A PROGRAM FOR WORKSPACE ANALYSIS	57

Chapter	Page
APPENDIX B - DETAILS OF THE ITERATIVE VELOCITY METHOD	61
APPENDIX C - LISTING OF A PROGRAM FOR JOINT DISPLACEMENT ANALYSIS USING THE ITERATIVE VELOCITY METHOD	64

LIST OF TABLES

Table		Page
I.	Effects of a_2 and α_3 on the Shape of a Cross-Section of the Workspace of 4R Robot Arms with $\alpha_1 = 90^\circ$, $\alpha_2 = 0$, $a_3 = a_4$, $S_1 = S_2 = S_3 = S_4 = 0$	13
II.	Effects of a_2 and α_2 on the Shape of a Cross-Section of the Workspace of 4R Robot Arms with $\alpha_1 = 90^\circ$, $\alpha_3 = 0$, $a_3 = a_4$, $S_1 = S_2 = S_3 = S_4 = 0$	14
III.	Effects of a_2 and α_3 on the Shape of a Cross-Section of the Workspace of 4R Robot Arms with $\alpha_1 = 90^\circ$, $\alpha_2 = 90^\circ$, $a_3 = a_4$, $S_1 = S_2 = S_3 = S_4 = 0$	15
IV.	Effects of a_2 and α_2 on the Shape of a Cross-Section of the Workspace of 4R Robot Arms with $\alpha_1 = 90^\circ$, $\alpha_3 = 90^\circ$, $a_3 = a_4$, $S_1 = S_2 = S_3 = S_4 = 0$	16
V.	Effects of α_2 , α_3 , a_1 , a_2 and a_3 on the Shape of a Cross-Section of the Workspace of 4R Robot Arms with $\alpha_1 = 90^\circ$, $a_3 > a_4$, $S_1 = S_2 = S_3 = S_4 = 0$	18
VI.	Summary of Results of Workspace Comparison for 4R Robots	20
VII.	Joint Displacements for the 'Popular' 3R Robot	25
VIII.	Examples of Joint Displacement Analysis Using the Iterative Velocity Method for 4R and 3R Robots	34

LIST OF FIGURES

Figure	Page
1. Relation between two Coordinate Systems	4
2. Link Parameters of Joints	4
3. The General 4R Robot	7
4. The 'Best' 3R Robot	9
5. Four Configurations of 4R Robot	12
6. 3R Robot Configuration for Joint Displacement Analysis . . .	23
7. The Plane Q with 3R Robot Arm	36
8. 3R Robot Arm with Space Constraints	37
9. Workarea of a Constrained 3R Robot, $a_2 = 3.5, a_3 = 3.5,$ $S_1 = 2.5$	39
10. Workarea of a Constrained 3R Robot, $a_2 = 3.75, a_3 = 3.25,$ $S_1 = 2.5$	40
11. Workarea of a Constrained 3R Robot, $a_2 = 4.0, a_3 = 3.0,$ $S_1 = 2.5$	41
12. Workarea of a Constrained 3R Robot, $a_2 = 4.5, a_3 = 2.5,$ $S_1 = 2.5$	42
13. Workarea of a Constrained 3R Robot, $a_2 = 3.5, a_3 = 3.5,$ $S_1 = 0$	43
14. Workarea of a Constrained 3R Robot, $a_2 = 3.75, a_3 = 3.25,$ $S_1 = 0$	44
15. Workarea of a Constrained 3R Robot, $a_2 = 4.0, a_3 = 3.0,$ $S_1 = 0$	45
16. Workarea of a Constrained 3R Robot, $a_2 = 4.2, a_3 = 2.8,$ $S_1 = 0$	46
17. Workarea of a Constrained 3R Robot, $a_2 = 4.19, a_3 = 4.19,$ $S_1 = 2.5$	48

Figure	Page
18. Workarea of a Constrained 3R Robot, $a_2 = 5.88$, $a_3 = 2.5$, $S_1 = 2.5$	49
19. Workarea of a Constrained 3R Robot, $a_2 = 5.38$, $a_3 = 3.0$, $S_1 = 2.5$	50
20. Workarea of a Constrained 4R Robot Arm	51
21. Sample Computer Output Showing the Workarea of a 4R Robot	60

NOMENCLATURE

a_i	- The length of the common normal between two joint axes z_i and z_{i+1}
A_i	- Coordinate transformation from system (i+1) to system i
C_i	- Plane i representing a space constraint
h	- Height of space constraint
H	- Pitch of the screw
L	- Length of space constraint
$\underline{L}_1, \underline{L}_2$	- Vectors fixed in the robot hand
\underline{n}	- Direction of the screw axis
$\underline{N}_1, \underline{N}_2$	- Vectors fixed in the robot hand, perpendicular to \underline{L}_1 and \underline{L}_2
O_i	- Origin of system i
$\underline{P}_1, \underline{P}_2$	- Vectors from origin of system to a point in the hand before and after change in position and orientation
Q	- A plane passing through the axis of the first joint of 3R robot and containing the second and third link
\underline{r}	- Normal from origin to screw axis
S	- Magnitude of translation
S_i	- Distance along the joint axes z_i from the common normal between x_{i-1} and x_i
t	- Time
\underline{V}	- Linear velocity

- \underline{W} - Vector related to angular velocity ($\underline{n} = \frac{\underline{W}}{|\underline{W}|}$)
- \underline{x}_i - Coordinates of a point in system i
- (x_e, y_e, z_e) - Coordinates of the robot hand (end position of arm)
- α_i - The angle between axis z_i and z_{i+1} , measured in a right-handed sense along the axis x_{i+1}
- θ_i - The angle measured in a right-handed sense along z_i axis, from a_{i-1} to a_i . This is the angle of rotation of the i^{th} link with respect to the $(i-1)^{\text{th}}$ link
- ϕ - Magnitude of rotation of the screw
- Δ - A small change in a variable

CHAPTER I

INTRODUCTION

1.1 Background

In the past few years, mechanical manipulators have been used heavily in the industry, especially with regard to parts handling and assembly. Attention has been given to the design of mechanical manipulators with respect to the number of degrees of freedom, and research has also been presented related to the workspace of manipulators. Various types of robots are in use in the industry; one of the more sophisticated ones is the so-called 6R robot, which is composed of six revolute joints. This type of robot will provide all the six degrees of freedom required for a rigid body motion. Even though the 6R robot is necessary for many of the complex operations encountered in the industry, it may be too complex and costly for various simpler tasks. In this study attention will be given to the robots that are suited for relatively simpler operations. Workspace, joint displacements and effects of space constraints on the workspace are the concepts of major concern to the robot designer.

Roth (1) presented some observations about the workspace of manipulators. He (2) later studied the influence of positioning the hand of the robot on the primary and total workspace (primary workspace is that portion of the total workspace within which each point can be

reached at any direction). Kumar and Waldron (3) presented an algorithm to plot the boundary contour of the workspace on a plane containing the base axis of the robot. Tsai and Soni (4) solved the accessible regions of robot arms for planar cases in closed-form. Tsai (4) has developed an algorithm to plot the boundary contours of the workspaces on any arbitrary plane. Pieper (5) presents a method to find joint displacements of a 6R manipulator containing three intersecting revolute axes, and numerical solutions for general 6R robots.

1.2 Objectives

It is proposed to compare the 3R and 4R manipulators. The added joint in the case of a 4R robot as compared to a 3R will effect the characteristics of the robot and it is of major concern in this study to find these effects. In other words, what are the gains in transition from 3R to 4R.

The objectives of this study are as follows:

1. To study the effects of manipulator parameters on the workspace of 4R robots, and compare the results with the 3R robots.
2. To compare the joint displacements of 3R and 4R robots for motion between two work stations. To develop a computer program using iterative velocity method as a possible tool to analyze the displacements of the robot joints.
3. To study the effects of space constraints on the workspace of 3R and 4R robots.

CHAPTER II

A COMPARISON OF THE WORKSPACES OF 3R AND 4R ROBOTS

2.1 Definition of the Workspace of a Robot Hand

The workspace of a robot hand is defined as the volume which contains all the accessible points of a robot hand. The concept of workspace is one of the most important characteristics of a manipulator. The objective of the robot designer is to establish a set of robot parameters so that the workspace becomes the largest possible fraction of a sphere with radius equal to the length of the robot in its extended position.

2.2 Mathematical Concepts for Workspace Analysis

In order to analyze the workspace of a manipulator a relation between the cartesian coordinate systems as shown in Figure 1 should be established. In this study the (4×4) matrix method developed by Denavit and Hartenberg (6) has been used.

The link parameters of a robot can be defined as follows (see Figure 2):

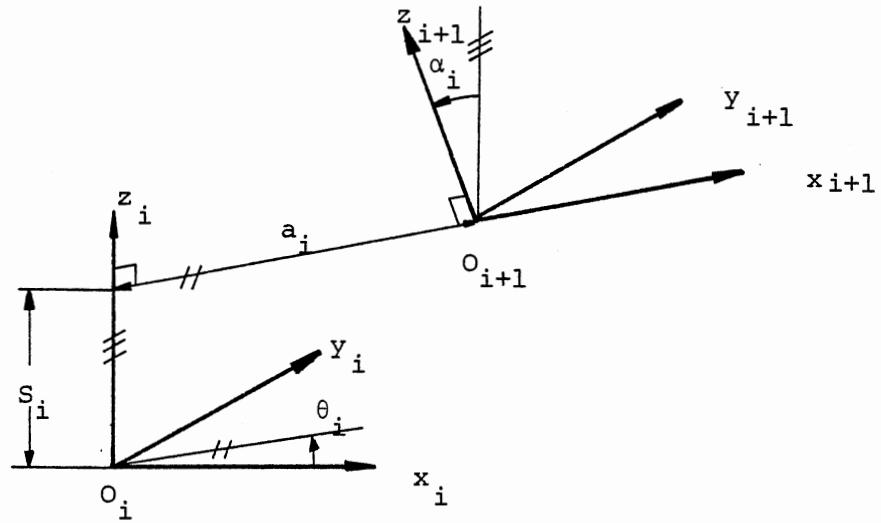


Figure 1. Relation between two Coordinate Systems

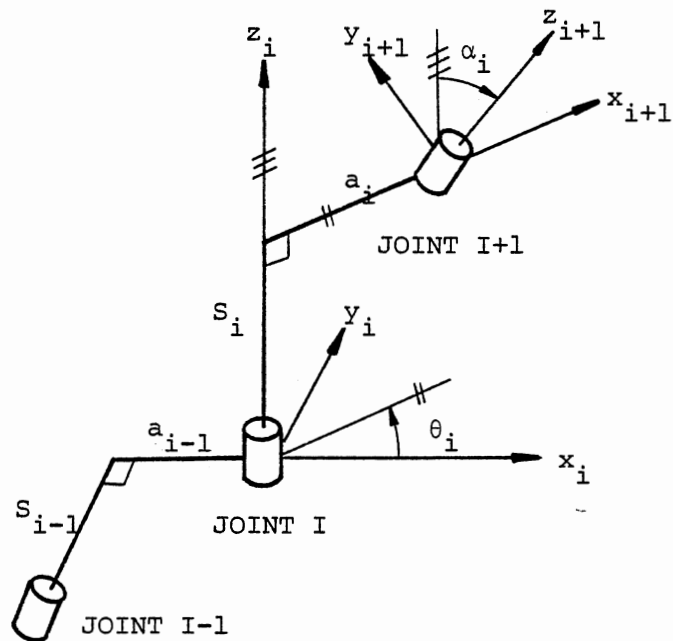


Figure 2. Link Parameters of Joints

- a_i : The length of the common normal between two joint axes, z_i and z_{i+1} .
- α_i : The angle between axis z_i and z_{i+1} , measured in a right-handed sense along the axis x_{i+1} .
- S_i : Distance along the joint axis z_i from the common normal between x_{i-1} and x_i .
- θ_i : The angle measured in a right-handed sense along z_i axis, from a_{i-1} to a_i . This is the angle of rotation of the i^{th} link with respect to the $(i-1)^{\text{st}}$ link.

The coordinates in the system i can be denoted by (x_i, y_i, z_i) and in system $(i+1)$ by $(x_{i+1}, y_{i+1}, z_{i+1})$. Then the vectors \underline{x}_i and \underline{x}_{i+1} can be defined so that

$$\underline{x}_i = \begin{bmatrix} x_i \\ y_i \\ z_i \\ 1 \end{bmatrix} \quad \underline{x}_{i+1} = \begin{bmatrix} x_{i+1} \\ y_{i+1} \\ z_{i+1} \\ 1 \end{bmatrix}$$

Then there is a transformation

$$\underline{x}_i = A_i \underline{x}_{i+1}$$

where

$$A_i = \begin{bmatrix} \cos \theta_i & -\sin \theta_i \cos \alpha_i & \sin \theta_i \sin \alpha_i & a_i \cos \theta_i \\ \sin \theta_i & \cos \theta_i \cos \alpha_i & -\cos \theta_i \sin \alpha_i & a_i \sin \theta_i \\ 0 & \sin \alpha_i & \cos \alpha_i & S_i \\ 0 & 0 & 0 & 1 \end{bmatrix} \quad (2.1)$$

For (n+1) coordinate systems there are (n) transformations between neighboring systems. A point represented by \underline{x}_{n+1} in system (n+1) can be represented with reference to system (1) as follows:

$$\underline{x}_1 = A_1 \cdot A_2 \cdot \dots \cdot A_n \underline{x}_{n+1} \quad (2.2)$$

For the 4R robot shown in Figure 3, equation 3.2 could be written as

$$\begin{bmatrix} x \\ y \\ z \\ 1 \end{bmatrix} = A_1 A_2 A_3 A_4 \begin{bmatrix} 0 \\ 0 \\ 0 \\ 1 \end{bmatrix} \quad (2.3)$$

Using Equation (3.3) the coordinate of the robot hand with respect to the fixed first coordinate system could be calculated.

2.3 Basic Considerations in Choosing the 'Right Robot'

According to research done by Tsai, the best 3R robot in terms of workspace has the following link parameters:

$$\begin{aligned} \alpha_1 &= 90^\circ & a_1 &= 0 \\ \alpha_2 &= 0^\circ & a_2 &= a_3 \\ s_1 &= s_2 = s_3 & &= 0 \end{aligned}$$

A 3R robot with link parameters as shown above will have the maximum workspace possible. In other words, the workspace for this specific robot is the total volume of a sphere with center at the origin or base point of the robot arm and a radius equal to the total sum of the link lengths. If the workspace of the robot is the only design criter-

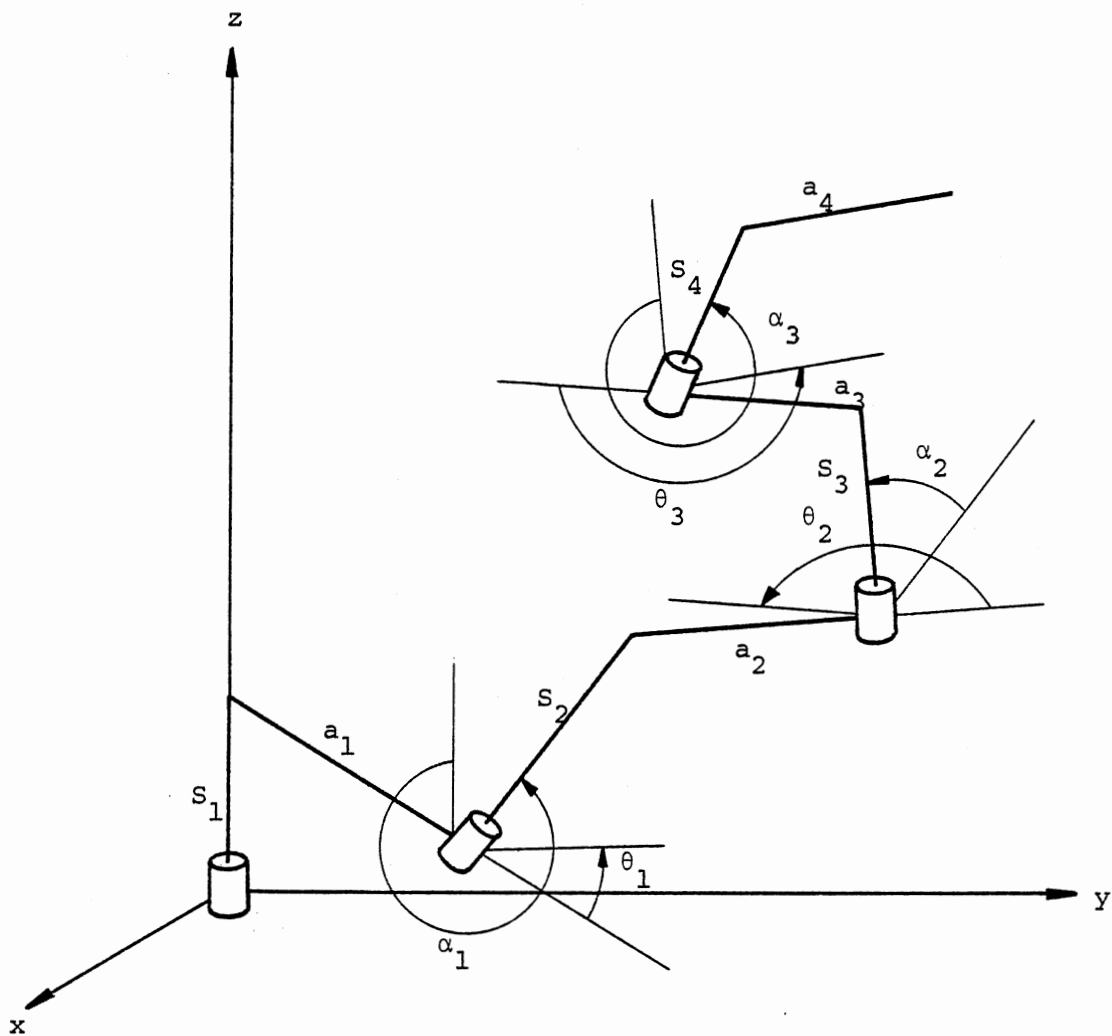


Figure 3. The General 4R Robot

ion, there is no need to employ a robot with more than 3 joints.

However, in many cases it is possible that the robot designer desires more degrees of freedom for the robot hand than the 3R robot can provide. In instances where all 6 degrees of freedom are required to perform the task, the solution is the sophisticated but complex 6R robot. However, many jobs do not require the full range of motion that the 6R can provide, so a simpler unit may be much more effective. A more complex robot will increase the degree of complexity in control and design, thus adding to the construction and maintenance cost of the unit. So, consideration of the 4R or 5R robots is quite worthwhile. The 4R robot could be ideal for some applications where it is required to control the direction of the robot hand for some limited ranges of motion. This is a task that can not be achieved by a 3R robot. Another limitation of the 3R robot is its lack of capability of obstacle avoidance. The 4R robot is more capable of avoiding obstacles in the path of motion. Therefore, many applications arise in practice where the 3 link robot is too limited, but a robot arm with 4 links is well suited.

2.4 The Type of Robot under Consideration

To analyze the workspace and displacements of each joint of a 6R robot, the structure of the robot has been divided in two parts. Milenkovic (7) divided the robot into 'major mechanism' and 'wrist mechanism'. The major mechanism provides the 'large range motion' of the robot arm, and the wrist mechanism provides the local motion of the robot hand. Tsai (8) has used the same division in his synthesis of

6R robots.

In this thesis, the 4R robot will be divided in two parts, each part having two joints. The first two joints have the same structure as the first two joints of the 'best' 3R robot, which is shown in Figure 4. The configuration of the first two joints will remain the same throughout this study ($\alpha_1 = 90^\circ$), as it provides the maximum range of motion for the third joint. The effect of changing the configuration of the remaining two joints will be studied here. In this case the first link length, a_1 , is equal to zero (see Figure 3), and the remaining three link lengths (a_2 , a_3 and a_4) are variable. The angle α_1 is 90° , α_2 and α_3 are variable. No offsets (S_1) have been introduced in the structure of the 4R robot being considered. This is because S_1 will only move the workspace of the robot hand up and down with respect to the x-y plane and will not change its shape. S_2 and S_3 in general will reduce the workspace and they can also cause voids (void is a volume within the workspace that the robot hand can not reach).

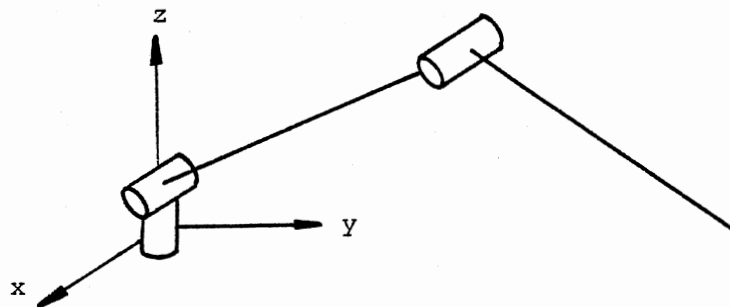


Figure 4. The 'Best' 3R Robot

2.5 Method of Analysis and Results

Consider the robot shown in Figure 3, which has four degrees of freedom by virtue of four revolute joints. The robot arm is free to rotate about joint 1 (z - axis) but θ_1 can be set equal to zero. θ_2 , θ_3 and θ_4 can each have the complete rotation 0° to 360° . Using Equation 2.3, all the points that can be reached by rotating joints 2, 3 and 4 can be found.

A polar projection about the first joint axes will represent the working area of the robot on the y-z plane. This polar projection is defined by the following mapping:

$$(x_1, y_1, z_1) \rightarrow (\sqrt{x_1^2 + y_1^2}, 0, z_1).$$

The total workspace of the robot arm can be obtained by rotating this projected area about the first joint axes. Therefore, the working area on the y-z plane is a good representation of the total manipulator workspace.

In order to compare the working area of the robots with different a and α values, the total link length of the compared robots should be the same. In this chapter each robot has a total link length of one.

The preceding method requires considerable amount of matrix manipulations. Therefore, the use of a computer to analyze the robot workspace in this way is necessary. A Fortran IV program was developed for the university's IBM 370 computer to carry out the necessary calculations. It makes use of the computer's printer plotting capability to show the working area on the y-z plane. A source listing of

the program and a sample of results are shown in Appendix A. The figures presented in the following pages are sketches of the printer plots obtained from this program.

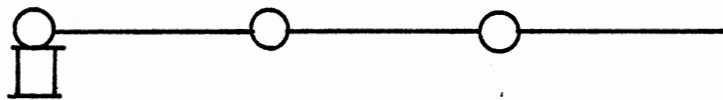
Figure 5 shows the four different configurations of the 4R robot that were considered. The orientation of the first two joints for all these cases is the same and only the orientation axes of the third and fourth joints will vary. In the first part of the study, four different combinations of robot link lengths were considered. They were as follows:

I -	$a_2 = 0.25$	$a_3 = a_4 = 0.375$
II -	$a_2 = 0.40$	$a_3 = a_4 = 0.30$
III -	$a_2 = 0.50$	$a_3 = a_4 = 0.25$
IV -	$a_2 = 0.60$	$a_3 = a_4 = 0.20$

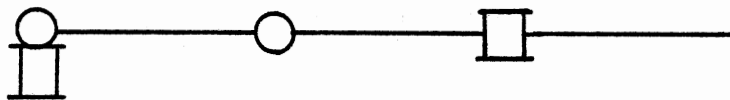
Table I presents the results obtained by varying α_3 from 0° to 90° and keeping $\alpha_1 = 90^\circ$, $\alpha_2 = 0^\circ$. This corresponds to a transition from case a) to case b) in Figure 5. It is immediately apparent from Table I that several of the robot configurations will have a workspace with some voids. As mentioned before it is the objective of the designer to create a robot that does not have voids in its workspace.

Table II presents results obtained by a transition from case a) to case c) in Figure 5. In a similar way, Table III shows results for a transition from case c) to case d) in Figure 5, and Table IV was obtained for a transition from case b) to case d).

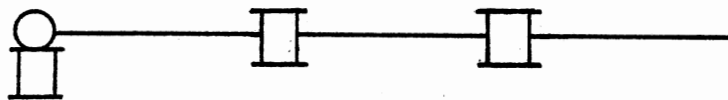
The second part of the study was done for the following combinations of link lengths:



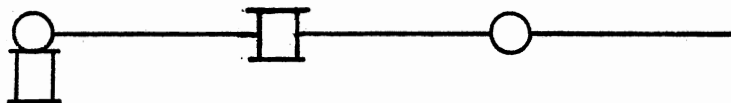
a) $\alpha_1 = 90^\circ, \alpha_2 = \alpha_3 = 0^\circ.$



b) $\alpha_1 = 90^\circ, \alpha_2 = 0^\circ, \alpha_3 = 90^\circ.$



c) $\alpha_1 = 90^\circ, \alpha_2 = 90^\circ, \alpha_3 = 0^\circ.$



d) $\alpha_1 = 90^\circ, \alpha_2 = 90^\circ, \alpha_3 = 90^\circ.$

Figure 5. Four Configurations of 4R Robots

TABLE I

EFFECTS OF a_2 AND α_3 ON THE SHAPE OF A CROSS-SECTION
OF THE WORKSPACE OF 4R ROBOT ARMS WITH

$$\alpha_1 = 90^\circ, \alpha_2 = 0, a_3 = a_4,$$

$$s_1 = s_2 = s_3 = s_4 = 0$$







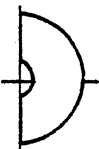
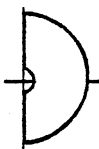
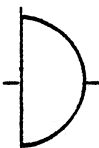




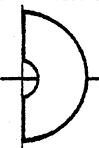


Case \ α_3	0	30	60	90
I				
II				
III				
IV				

TABLE II

EFFECTS OF a_2 AND α_2 ON THE SHAPE OF A CROSS-SECTION
OF THE WORKSPACE OF 4R ROBOT ARMS WITH

$$\alpha_1 = 90^\circ, \alpha_3 = 0, a_3 = a_4,$$

$$S_1 = S_2 = S_3 = S_4 = 0$$

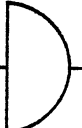
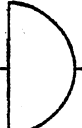
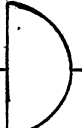
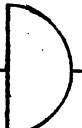
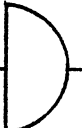
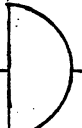


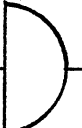
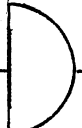

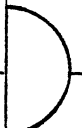



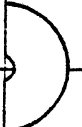
α_2	0	30	60	90
Case				
I				
II				
III				
IV				

TABLE III

EFFECTS OF a_2 AND α_3 ON THE SHAPE OF A CROSS-SECTION OF THE WORKSPACE OF 4R ROBOT ARMS WITH

$$\alpha_1 = 90^\circ, \alpha_2 = 90^\circ, a_3 = a_4,$$

$$s_1 = s_2 = s_3 = s_4 = 0$$


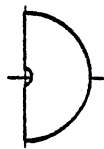
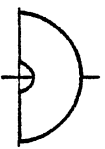

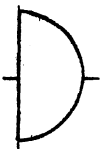

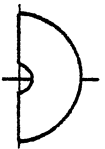
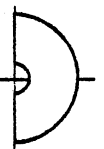
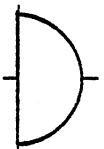
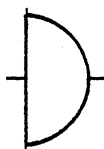


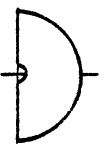
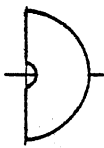
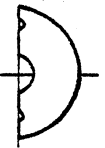









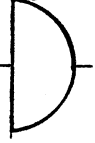
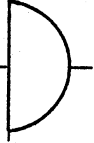
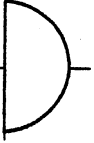





α_3	0	30	60	90
Case				
I				
II				
III				
IV				

TABLE IV

EFFECTS OF a_2 AND α_2 ON THE SHAPE OF A CROSS-SECTION
OF THE WORKSPACE OF 4R ROBOT ARMS WITH

$$\alpha_1 = 90^\circ, \alpha_3 = 90^\circ, a_3 = a_4,$$

$$s_1 = s_2 = s_3 = s_4 = 0$$

α_2	0	30	60	90
Case				
I				
II				
III				
IV				

A -	$a_2 = 0.25$	$a_3 = 0.45$	$a_4 = 0.30$
B -	$a_2 = 0.35$	$a_3 = 0.35$	$a_4 = 0.30$
C -	$a_2 = 0.50$	$a_3 = 0.35$	$a_4 = 0.15$
D -	$a_2 = 0.60$	$a_3 = 0.30$	$a_4 = 0.10$

In all cases considered, $a_3 > a_4$. The results for these sets of parameters are presented in Table V.

From Table I it can be seen that for a robot with $\alpha_1 = 90^\circ$, $\alpha_2 = 0^\circ$ and $\alpha_3 = 0^\circ$ (case a) from Figure 5), workarea is always a half circle until a_2 becomes larger than $(a_3 + a_4)$. A workarea of half circle represents the maximum obtainable workspace for the robot hand. As α_3 is changed from 0° to 90° in Table I, it is seen that only for case III ($a_2 = 2a_3 = 2a_4$) the workspace is a complete half circle. Therefore, unless the robot has $\alpha_1 = 90^\circ$, $\alpha_2 = \alpha_3 = 0^\circ$, there will be severe restrictions on the relative link lengths of the robot arm.

From Table II it is apparent that in the transition from case a) to case c) (in Figure 5), all of the cases will provide a complete half circle workarea, except case IV, for which $a_2 > a_3 + a_4$.

Table III shows the transition from case c) to case d). The only combination of link lengths to give the complete half circle workarea is case III ($a_2 = 2a_3 = 2a_4$). The same situation occurs in Table IV, where there is a transition from case b) to case d) in Figure 5. The only good set of link lengths is $a_2 = 2a_3 = 2a_4$.

The results from the second part of this study (Table V), show that for the cases where $a_3 > a_4$, the best orientations of the joints are cases a) and c) from Figure 5. The limitation on these

TABLE V

EFFECTS OF α_2 , α_3 , a_1 , a_2 AND a_3 ON THE SHAPE OF
A CROSS-SECTION OF THE WORKSPACE OF 4R ROBOT

ARMS WITH $\alpha_1 = 90^\circ$, $a_3 > a_4$,

$$S_1 = S_2 = S_3 = S_4 = 0$$

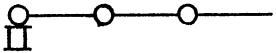
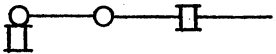
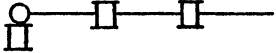
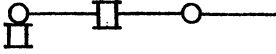
Case Angles	A	B	C	D
$\alpha_1 = 90^\circ$ $\alpha_2 = 0^\circ$ $\alpha_3 = 0^\circ$				
$\alpha_1 = 90^\circ$ $\alpha_2 = 0^\circ$ $\alpha_3 = 90^\circ$				
$\alpha_1 = 90^\circ$ $\alpha_2 = 90^\circ$ $\alpha_3 = 0^\circ$				
$\alpha_1 = 90^\circ$ $\alpha_2 = 90^\circ$ $\alpha_3 = 90^\circ$				

configurations is that the second link should not be longer than the sum of third and fourth links.

These results are summarized in Table VI. It has been shown that the best 4R robot configurations in terms of workspace are cases a) and c) in Table VI.

TABLE VI

SUMMARY OF RESULTS OF WORKSPACE
COMPARISON FOR 4R ROBOTS

Case	Results
a) 	<u>No voids</u> for all the linklength combinations, <u>except</u> when $a_2 > a_3 + a_4$.
b) 	<u>Voids</u> for all the linklength combinations, <u>except</u> when $a_2 = a_3 + a_4$.
c) 	<u>No voids</u> for all the linklength combinations, <u>except</u> when $a_2 > a_3 + a_4$.
d) 	<u>Voids</u> for all the linklength combinations, <u>except</u> when $a_2 = 2a_3 = 2a_4$.

CHAPTER III

JOINT DISPLACEMENT ANALYSIS

3.1 Introduction

One of the major concerns of the robot designer is the motion of all the robot joints. It is important to minimize the joint displacements of the robot in order to reduce energy consumption and maintenance cost. The problem of finding the displacements of each joint involves solving complex simultaneous algebraic equations. This process becomes more tedious as the number of joints of the robot increases. Several analytical and numerical methods have been developed to study the joint motion of some specific robot configurations.

A closed-form solution can be obtained for specific 3R robots. In this study, a closed-form solution for the 'popular' 3R robot ($\alpha_1 = 90^\circ$, $\alpha_2 = 0$, $\alpha_3 = 0$, $a_1 = 0$, $a_2 = a_3$) will be presented. Two numerical methods, the Newton-Raphson and the iterative velocity method (developed by Pieper (5)) have been applied successfully to general 6R robots. In this chapter the iterative velocity method will be applied to find joint displacements of robots with fewer degrees of freedom.

3.2 A Comparison of Joint Displacements of the 'Popular' 3R Robot and General 4R Robots

A closed-form solution can be obtained from the geometry of the 3R robot with the parameters $\alpha_1 = 90^\circ$, $\alpha_2 = \alpha_3 = 0$, $a_1 = 0$, $S_2 = S_3 = 0$. Figure 6 shows the configuration of this 3R robot and it can be verified that the joint variables θ_i , $i = 1, 2, 3$ are as follows:

$$\theta_1 = \tan^{-1}(y_e/x_e) \quad (3.1)$$

$$\theta_2 = \cos^{-1} \frac{z_e - S_1}{L} - \cos^{-1} \frac{L^2 + (a_2^2 - a_3^2)}{2a_2 L} \quad (3.2)$$

$$\theta_3 = \cos^{-1} \frac{L^2 - (a_2^2 - a_3^2)}{2a_2 a_3} \quad (3.3)$$

where

$$L = \{(x_e)^2 + (y_e)^2 + (z_e - S_1)^2\}^{1/2}.$$

Given the coordinates of the robot hand (end position of the robot), Equations (3.1) through (3.3) can be used to find the joint variables.

The following procedure will be used for comparison of joint displacements of the 3R and 4R robots:

1. For given 4R robot parameters and a given set of joint variables, Equation (2.3) can be used to find the corresponding position of the hand (work station). Two work stations can be obtained with two sets of joint variables.

2. For a given 3R robot, the joint variables corresponding to

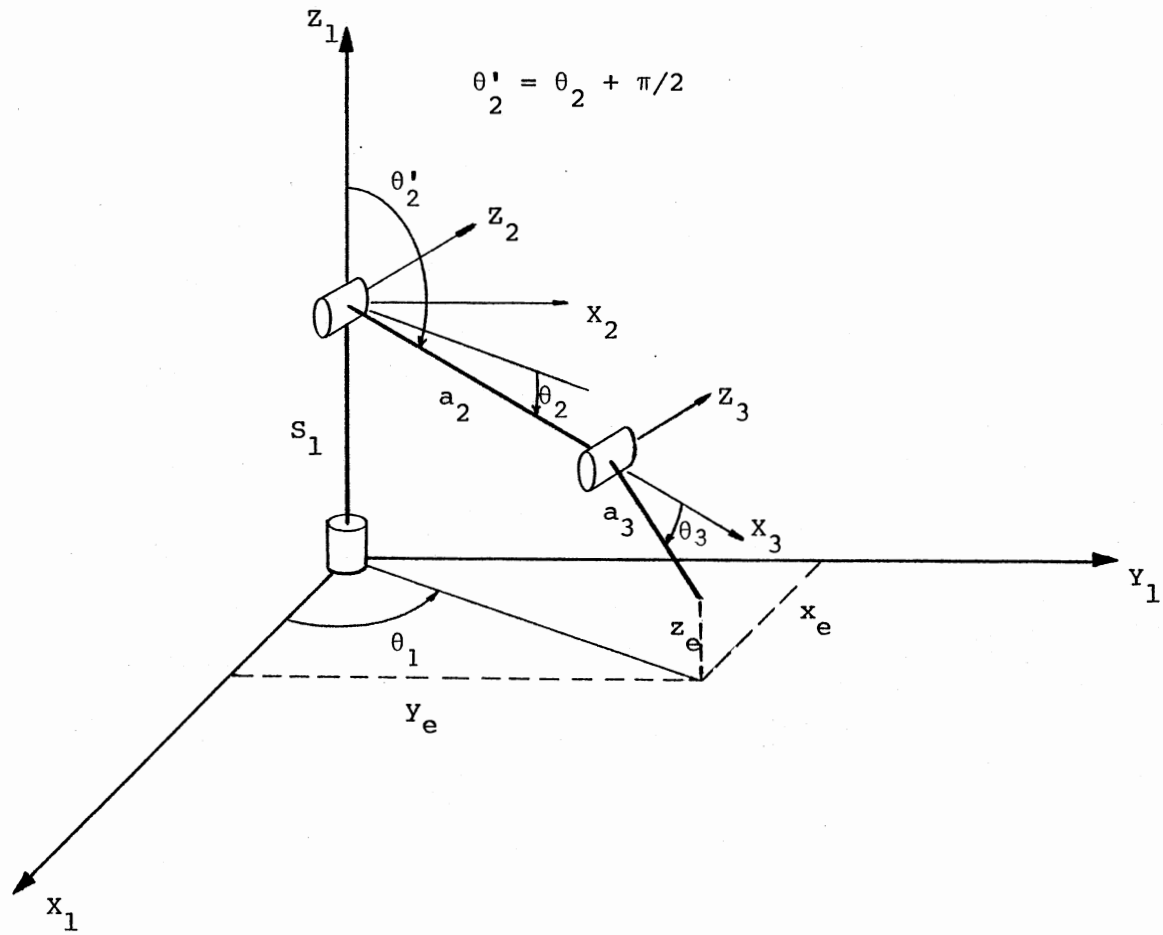


Figure 6. 3R Robot Configuration for Joint Displacement Analysis

the same workstation as in 1. can be found from Equations (3.1) through (3.3).

3. Joint displacements of 3R and 4R robots in going from station one to station two can then be found.

In this comparison the 'popular' 3R robot will be compared to the 4R robots shown in Figure 5. The total linklength of all robots being compared is one. For the 4R robots, $a_2 = 0.5$, $a_3 = a_4 = 0.25$. The following sets of joint variables of the 4R robots were chosen:

<u>Set One</u>	<u>Set Two</u>	<u>Joint Displacement</u>
$\theta_1 = -30.0$	$\theta_1 = 20.0$	$\Delta\theta_1 = 50.0$
$\theta_2 = 40.0$	$\theta_2 = 80.0$	$\Delta\theta_2 = 40.0$
$\theta_3 = -35.0$	$\theta_3 = 155.0$	$\Delta\theta_3 = 170.0$
$\theta_4 = -95.0$	$\theta_4 = 70.0$	$\Delta\theta_4 = 165.0$

A computer program based on Equation (2.3) was used to find the coordinates of the corresponding work stations for the four different 4R robots. Table VII shows the resulting joint displacements for the 'popular' 3R robot.

The results from Table VII indicate that the total sum of joint displacements for the 4R robot is higher in all the cases considered. However, the joint displacements of first and second joints have much more effect on the energy consumption. This is because of the load, which will be much more for the first and second joints than the third and fourth joints. The 4R robot with parameters $\alpha_1 = 90^\circ$, $\alpha_2 = 90^\circ$,

TABLE VII
 JOINT DISPLACEMENTS FOR THE 'POPULAR' 3R ROBOT

4R Robot Configurations	4R Robot Joint Displacements	Corresponding Joint Displacements of the 'Popular' 3R
$\alpha_1 = 90^\circ$	$\Delta\theta_1 = 50^\circ$	$\Delta\theta_3 = 50.0^\circ$
$\alpha_2 = 0^\circ$	$\Delta\theta_2 = 40^\circ$	$\Delta\theta_2 = 68.0^\circ$
$\alpha_3 = 0^\circ$	$\Delta\theta_3 = 170^\circ$	$\Delta\theta_3 = 65.7^\circ$
	$\Delta\theta_4 = 165^\circ$	
$\alpha_1 = 90^\circ$	$\Delta\theta_1 = 50^\circ$	$\Delta\theta_1 = 93.6^\circ$
$\alpha_2 = 0^\circ$	$\Delta\theta_2 = 40^\circ$	$\Delta\theta_2 = 41.0^\circ$
$\alpha_3 = 90^\circ$	$\Delta\theta_3 = 170^\circ$	$\Delta\theta_3 = 56.6^\circ$
	$\Delta\theta_4 = 165^\circ$	
$\alpha_1 = 90^\circ$	$\Delta\theta_1 = 50^\circ$	$\Delta\theta_1 = 92.0^\circ$
$\alpha_2 = 90^\circ$	$\Delta\theta_2 = 40^\circ$	$\Delta\theta_2 = 52.1^\circ$
$\alpha_3 = 0^\circ$	$\Delta\theta_3 = 170^\circ$	$\Delta\theta_3 = 65.7^\circ$
	$\Delta\theta_4 = 165^\circ$	
$\alpha_1 = 90^\circ$	$\Delta\theta_1 = 50^\circ$	$\Delta\theta_1 = 2.21^\circ$
$\alpha_2 = 90^\circ$	$\Delta\theta_2 = 40^\circ$	$\Delta\theta_2 = 3.38^\circ$
$\alpha_3 = 90^\circ$	$\Delta\theta_3 = 170^\circ$	$\Delta\theta_3 = 56.6^\circ$
	$\Delta\theta_4 = 165^\circ$	

$\alpha_3 = 0$ has considerably less joint displacements for the first two joints than the 'popular' 3R robot. So, in terms of energy consumption it will perform better than the 'popular' 3R robot. The third and fourth joints of this 4R robot ($\alpha_1 = 90^\circ$, $\alpha_2 = 90^\circ$, $\alpha_3 = 0$) have considerably higher joint displacements but the energy consumption of these joints is much lower than the base joints.

In general, the joint displacements of a robot will be affected by the initial and final locations of the robot hand. This indicates that the location of the robot in its working space is important in terms of minimizing the joint displacements required during its operation. It is therefore necessary for the designer to have a tool for analyzing joint motions of a robot, so that the 'best' arrangement of the robot and its work stations can be achieved. Section 3.3 presents the iterative velocity method for joint displacement analysis developed by Pieper (5).

3.3 The Iterative Velocity Method

The iterative velocity method is based on the fact that a change in position and orientation of a rigid body can be described by a screw motion. The rotation and translation of this motion is along a single fixed axis. For small motion, the screw is related to the angular velocity of the rigid body.

Any rigid body can be defined in a coordinate system by two vectors located on the rigid body and a vector from the origin of the reference axis to a point on the rigid body. The screw motion is a way of defining the motion of a rigid body in reference to a fixed

coordinate system, when the body moves from one position to another.

The following terminology will be used:

\underline{L}_1 and \underline{N}_1 : Two vectors fixed in the robot hand in its initial state.

\underline{L}_2 and \underline{N}_2 : The same two vectors after a change in position and orientation.

\underline{P}_1 and \underline{P}_2 : Vectors from the origin of the system to the same point in the hand before and after the change in position and orientation.

\underline{r} : The normal from the origin to the screw axis.

\underline{n} : The direction of the screw axis.

ϕ : The magnitude of rotation of the screw.

S : The magnitude of the translation.

H : The pitch of the screw.

The direction of the screw axis \underline{n} and the magnitude of the rotation ϕ can be found from the following statement of Euler's theorem:

$$\underline{n} \tan(\phi/2) = \frac{(\underline{L}_2 - \underline{L}_1) \times (\underline{N}_2 - \underline{N}_1)}{(\underline{L}_2 - \underline{L}_1) \cdot (\underline{N}_2 + \underline{N}_1)} .$$

Define

$$\underline{W} = \frac{(\underline{L}_2 - \underline{L}_1) \times (\underline{N}_2 - \underline{N}_1)}{(\underline{L}_2 - \underline{L}_1) \cdot (\underline{N}_2 + \underline{N}_1)} .$$

Then

$$\underline{n} = \frac{\underline{W}}{|\underline{W}|} .$$

$$\phi = 2 \arctan |\underline{W}| .$$

The normal from the origin to the screw axis, \underline{r} , is computed from

$$\underline{r} = \frac{1}{2} \left\{ \underline{P}_1 + \underline{P}_2 + \underline{W} \times \frac{(\underline{P}_2 - \underline{P}_1)}{|\underline{W}|^2} - \underline{W} \cdot \frac{(\underline{P}_2 + \underline{P}_1)}{|\underline{W}|^2} \times \underline{W} \right\} .$$

The magnitude of the translation S is

$$S = \left| \frac{\underline{W} \cdot (\underline{P}_2 - \underline{P}_1)}{|\underline{W}|} \right| .$$

Lastly, the pitch of the screw H is defined as

$$H = \frac{S}{\phi} .$$

The preceding defines all the necessary parameters of the screw.

\underline{W} and \underline{V} can be written as approximations respectively to the angular velocity of the hand and the linear velocity of a point in the hand at the origin:

$$\underline{W} = \frac{\Delta\phi}{\Delta t} \underline{n} \quad (3.4)$$

$$\underline{V} = H \frac{\Delta\phi}{\Delta t} \underline{n} - \underline{n} \times \underline{r} \frac{\Delta\phi}{\Delta t} \quad (3.5)$$

where the quantities on the right-hand sides of the above equations are found from the screw; $\Delta\phi$ is the amount of rotation, \underline{n} is a unit vector parallel to the screw axis, H is the pitch of the screw, and \underline{r} is a

vector from the origin to the screw axis. The details regarding Equations (3.4) and (3.5) are shown in Appendix B. In addition, the angular and linear velocities may be expressed as functions of the rotations in the arm joints. That is

$$\underline{W} = \sum_{i=1}^6 \underline{W}_i \quad (3.6)$$

$$\underline{V} = - \sum_{i=1}^6 \underline{W}_i \times \underline{r}_i \quad (3.7)$$

where \underline{W}_i is the angular velocity of the hand due to the rotation about axis (i) and \underline{r}_i is a vector from the origin of system 1 to the axis (i).

The following approximation can be made:

$$\underline{W}_i \approx \frac{\Delta\phi}{\Delta t} \underline{n}_i \quad (i = 1, 2, \dots, 6) \quad (3.8)$$

where \underline{n}_i is a unit vector parallel to axis (i) and it is assumed that the motion of the hand from initial to final position is small, so that Equations (3.6) and (3.7) may be written using Equation (3.8) as

$$\underline{W} = \sum_{i=1}^6 \frac{\Delta\phi_i}{\Delta t} \underline{n}_i \quad (3.9)$$

$$\underline{V} = - \sum_{i=1}^6 \frac{\Delta\phi_i}{\Delta t} \underline{n}_i \times \underline{r}_i \quad (3.10)$$

Then, equating the right hand sides of Equations (3.9) and (3.10) to the right hand sides of Equations (3.4) and (3.5), two vector

equations representing six scalar linear equations in θ_i , $i = 1, \dots, 6$ can be obtained. Equating and dividing by Δt yields

$$\sum_{i=1}^6 (\Delta\theta_i \underline{n}_i) = \Delta\phi \underline{n} \quad (3.11)$$

$$- \sum_{i=1}^6 (\Delta\theta_i \underline{n}_i \times \underline{r}_i) = H \Delta\phi \underline{n} - \underline{n} \times \underline{r} \Delta\phi. \quad (3.12)$$

Equations (3.11) and (3.12) can be used iteratively to approximate the joint displacements θ_i in going from one position of the robot hand to another. However, they are valid only for a small change in the screw angle $\Delta\phi$. If the required motion of the hand is large, it can be divided into smaller steps so that the right-hand sides of Equations (3.11) and (3.12) stay within reasonable limits.

An initial and a final position of the robot hand are given. From the initial configuration the vectors \underline{n}_i and \underline{r}_i can be found. If they are not within their limits, then a new 'intermediate' final position is found. This intermediate position and the initial position are used to obtain $\Delta\phi$, \underline{n} and \underline{r} and the joint displacements, $\Delta\theta_i$, can be found from Equations (3.11) and (3.12). The 'intermediate' position now becomes the new initial position and the same process is carried through until the final position is reached. The total displacements of each joint can then be found. Therefore, for large motions, only a portion of the screw should be used to compute the incremental change in the angles. The change that is made at each iteration should also be limited.

A computer program has been written utilizing the above scheme; a source listing is included in Appendix C. Section 3.4 presents examples of joint displacement analysis using the above mentioned program.

3.4 Examples of Joint Displacement Analysis

In this section three examples of joint displacement analysis for 6R, 4R and 3R robots will be presented. The first example is for a 6R robot. The link parameters of this 6R robot are as follows:

$$s_1 = s_2 = s_3 = s_4 = s_5 = s_6 = 0.0$$

$$a_1 = 0.0 \qquad \alpha_1 = 90.0$$

$$a_2 = 2.0 \qquad \alpha_2 = 0.0$$

$$a_3 = 2.0 \qquad \alpha_3 = -90.0$$

$$a_4 = 1.0 \qquad \alpha_4 = 90.0$$

$$a_5 = 0.5 \qquad \alpha_5 = -90.0$$

$$a_6 = 0.3 \qquad \alpha_6 = 0.0$$

The target hand positions were generated by sets of known angles. The initial position of the robot hand was generated by the angles

$$\theta_1 = 60.0^\circ \qquad \theta_4 = 20.0^\circ$$

$$\theta_2 = 40.0^\circ \qquad \theta_5 = 50.0^\circ$$

$$\theta_3 = 30.0^\circ \qquad \theta_6 = 70.0^\circ$$

This leads to the hand position specified by the position vector

$$\underline{P}_1 = \begin{bmatrix} 0.45728 \\ 2.27080 \\ 4.45730 \end{bmatrix}$$

and the orientation (specified by two unit vectors fixed in the hand \underline{L}_1 pointing in the direction of the hand and \underline{N}_1 in the direction of the sixth revolute axis)

$$\underline{L}_1 = \begin{bmatrix} -0.97257 \\ 0.23188 \\ -0.01827 \end{bmatrix} \quad \underline{N}_1 = \begin{bmatrix} -0.19821 \\ 0.86732 \\ 0.45659 \end{bmatrix}$$

The target was generated by the angles

$$\begin{aligned} \theta_1 &= 65.000^\circ & \theta_4 &= 30.000^\circ \\ \theta_2 &= 45.000^\circ & \theta_5 &= 40.000^\circ \\ \theta_3 &= 40.000^\circ & \theta_6 &= 100.000^\circ \end{aligned}$$

with

$$\underline{P}_2 = \begin{bmatrix} -0.2530 \\ 1.6519 \\ 4.4433 \end{bmatrix} \quad \underline{L}_2 = \begin{bmatrix} 0.68807 \\ 0.38511 \\ -0.61502 \end{bmatrix} \quad \underline{N}_2 = \begin{bmatrix} -0.05173 \\ -0.87143 \\ -0.48779 \end{bmatrix}$$

The results of the iterative velocity method for the joint angles of the target position were found as follows:

$$\begin{aligned} \theta_1 &= 64.996^\circ & \theta_4 &= 30.008^\circ \\ \theta_2 &= 45.004^\circ & \theta_5 &= 40.003^\circ \\ \theta_3 &= 39.995^\circ & \theta_6 &= 99.993^\circ \end{aligned}$$

The above results were obtained by 203 iterations.

In order to use the velocity method for 4R and 3R robot arms, four and three of the six equations available from Equations (3.11) and (3.12) respectively will be used. Table VIII shows the two examples for 3R and 4R robots.

TABLE VIII

EXAMPLES OF JOINT DISPLACEMENT ANALYSIS
 USING THE ITERATIVE VELOCITY METHOD
 FOR 4R AND 3R ROBOTS

Type of Robot	Link Parameters	Joint Angles for Initial Position	Joint Angles for Target Position	Results of Velocity Method for Joint Angles	Number of Iterations
4R	$s_1 = s_2 = s_3 = s_4 = 0$ $a_1 = 0.0 \quad \alpha_1 = 90.0^{\circ}$ $a_2 = 0.50 \quad \alpha_2 = -90.0^{\circ}$ $a_3 = 0.25 \quad \alpha_3 = 0.0^{\circ}$ $a_4 = 0.25 \quad \alpha_4 = 0.0^{\circ}$	$\theta_1 = 0.0^{\circ}$ $\theta_2 = 45.0^{\circ}$ $\theta_3 = 0.0^{\circ}$ $\theta_4 = 0.0^{\circ}$	$\theta_1 = -20.0^{\circ}$ $\theta_2 = 80.0^{\circ}$ $\theta_3 = -40.0^{\circ}$ $\theta_4 = 45.0^{\circ}$	$\theta_1 = -20.0^{\circ}$ $\theta_2 = 80.0^{\circ}$ $\theta_3 = -40.0^{\circ}$ $\theta_4 = 45.0^{\circ}$	193
3R	$s_1 = s_2 = s_3 = 0$ $a_1 = 0.0 \quad \alpha_1 = 90.0^{\circ}$ $a_2 = 0.50 \quad \alpha_2 = -90.0^{\circ}$ $a_3 = 0.50 \quad \alpha_3 = 0.0^{\circ}$	$\theta_1 = 0.0^{\circ}$ $\theta_2 = 45.0^{\circ}$ $\theta_3 = 0.0^{\circ}$	$\theta_2 = -10.0^{\circ}$ $\theta_2 = 55.0^{\circ}$ $\theta_3 = 20.0^{\circ}$	$\theta_1 = -10.0^{\circ}$ $\theta_2 = 55.0^{\circ}$ $\theta_3 = 20.0^{\circ}$	43

CHAPTER IV

THE EFFECT OF SPACE CONSTRAINTS ON THE WORKSPACE OF 3R AND 4R ROBOTS

4.1 Introduction

In practice, when a manipulator has been installed, the motion of its arm can be constrained by the surrounding walls, ceiling, floor etc. When the links are no longer free to move in all directions, the workspace of the robot hand can be greatly affected. As mentioned in Chapter II, certain configurations of 3R and 4R robots are 'best' in terms of workspace, if no space constraints are present. If space constraints are introduced, these 'best' robots may no longer provide the maximum workspace. This chapter introduces a brief analysis of how space constraints can affect the workspace of certain 3R and 4R robots.

4.2 Workspace Analysis in the Presence of

Space Constraints

The introduction of space constraints around the manipulator will make the problem of workspace analysis far more complex. A method needs to be developed that will find the position of the hand for the allowable motion range of the joints. Because of the complexity of this problem, this study will be confined to analyzing the workspace of

the 'popular' 3R robot ($S_1 = S_2 = S_3 = 0$, $a_1 = 0$, $a_2 = a_3$, $\alpha_1 = 90^\circ$, $\alpha_2 = \alpha_3 = 0$) and the effect of varying its link lengths a_2 and a_3 , and with introducing an offset S_1 . The effects of space constraints on a 4R robot with link parameters $S_1 = S_2 = S_3 = S_4 = 0$, $a_1 = 0$, $\alpha_1 = 90^\circ$, $\alpha_2 = \alpha_3 = \alpha_4 = 0$ will also be discussed. Figure 7 shows the 3R robot with space constraints represented by planes C_1 through C_6 . In this case, since the second joint and the third joint have parallel axes, the characteristic of the workspace affected by the space constraints can be studied on the plane passing through the axis of first joint and containing link two and three. This plane is shown by plane Q in Figure 7. Plane Q and the 3R robot arm are shown in Figure 8.

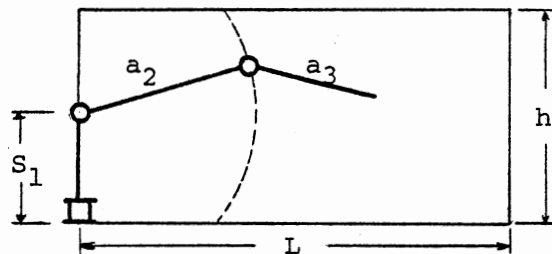


Figure 7. The Plane Q with 3R Robot Arm

The workspace analysis presented here was done using Tektronix graphics. The second joint of the robot arm is rotated through its full allowable range of motion, the dotted line in Figure 8 shows the path generated by the third joint. For a finite number of points on the

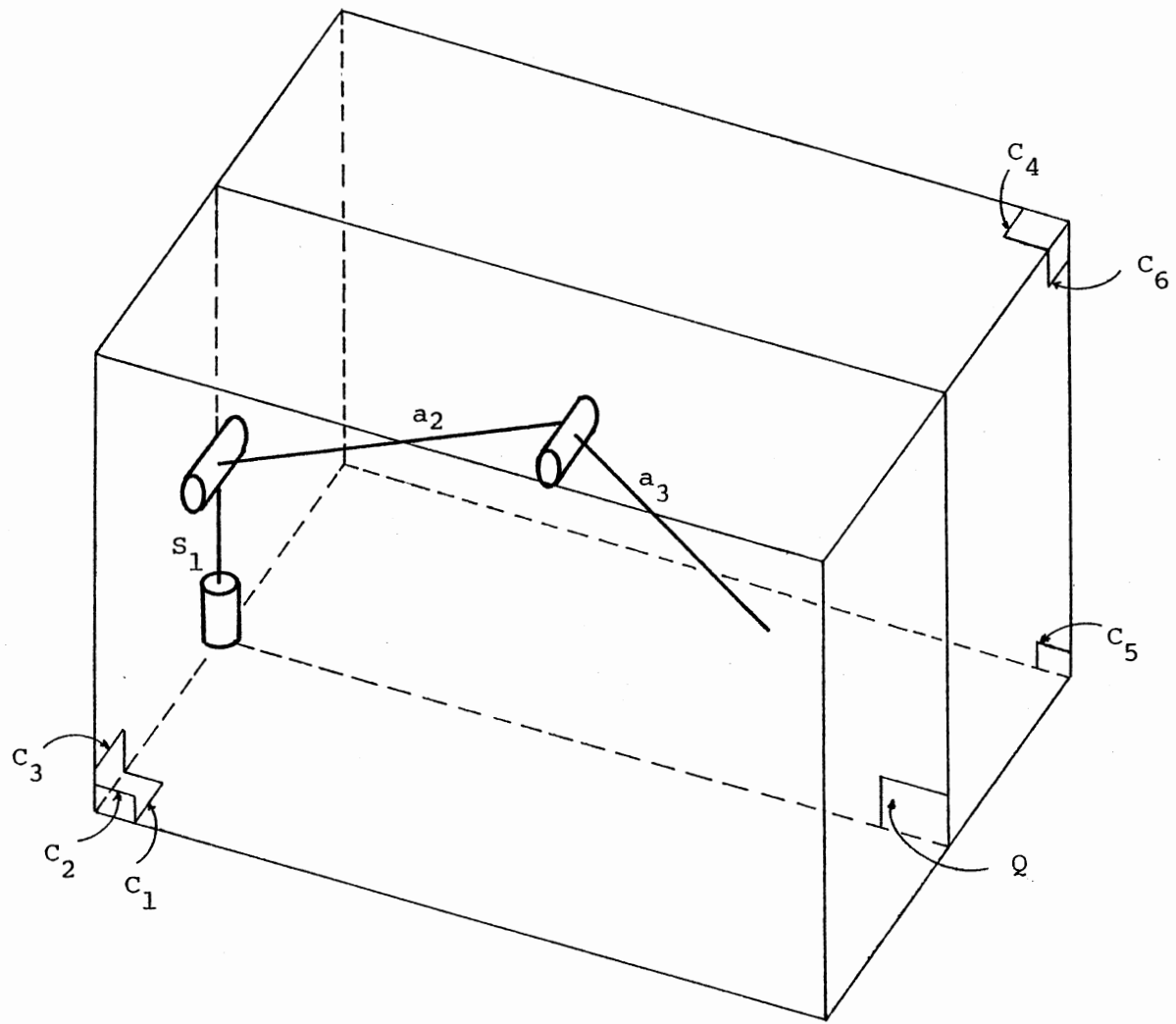


Figure 8. 3R Robot Arm with Space Constraints

dotted line the third joint is rotated through 360° , thus going through more than the allowable work area of the hand. A 'virtual window' corresponding to the location of the constraints is defined using Tektronix routines, so that only the workarea within the constraints is shown.

Three groups of 3R robots were considered. The robots in the first group all had an offset $S_1 = 2.5$ (note that the second joint is located at $h/2$). The constraints imposed on the robot motion correspond to dimensions of the plane Q defined in Figure 8 by $h = 5$ and $L = 8$. The total sum of the link lengths $a_2 + a_3 = 7$. The results are shown in Figures 9 through 12. Looking at Figure 9, it is seen that this robot configuration has a large void in the middle of the workarea. In Chapter II it was discussed that this configuration of the robot gives the maximum workspace without any voids, when there are no constraints on the link motion. Figure 10 shows a workarea with a smaller void in the middle, but the robot hand can not reach within a small area around joint two. As a_4 is made smaller compared to a_3 , the void in the middle of the workarea gets smaller until it disappears for $a_4 = S_1$, as shown in Figure 12. The robot represented in Figure 12, even though it has an unaccessible region by the left side of the constrained area, it is more desirable because it has a continuous workspace. Therefore, when constraints have been introduced, the 'popular' 3R robot will not produce the maximum workspace.

Figures 13 through 16 show the workarea of 3R robots with zero offset ($S_1 = 0$). Figure 13 shows the workarea of the 'popular' 3R.

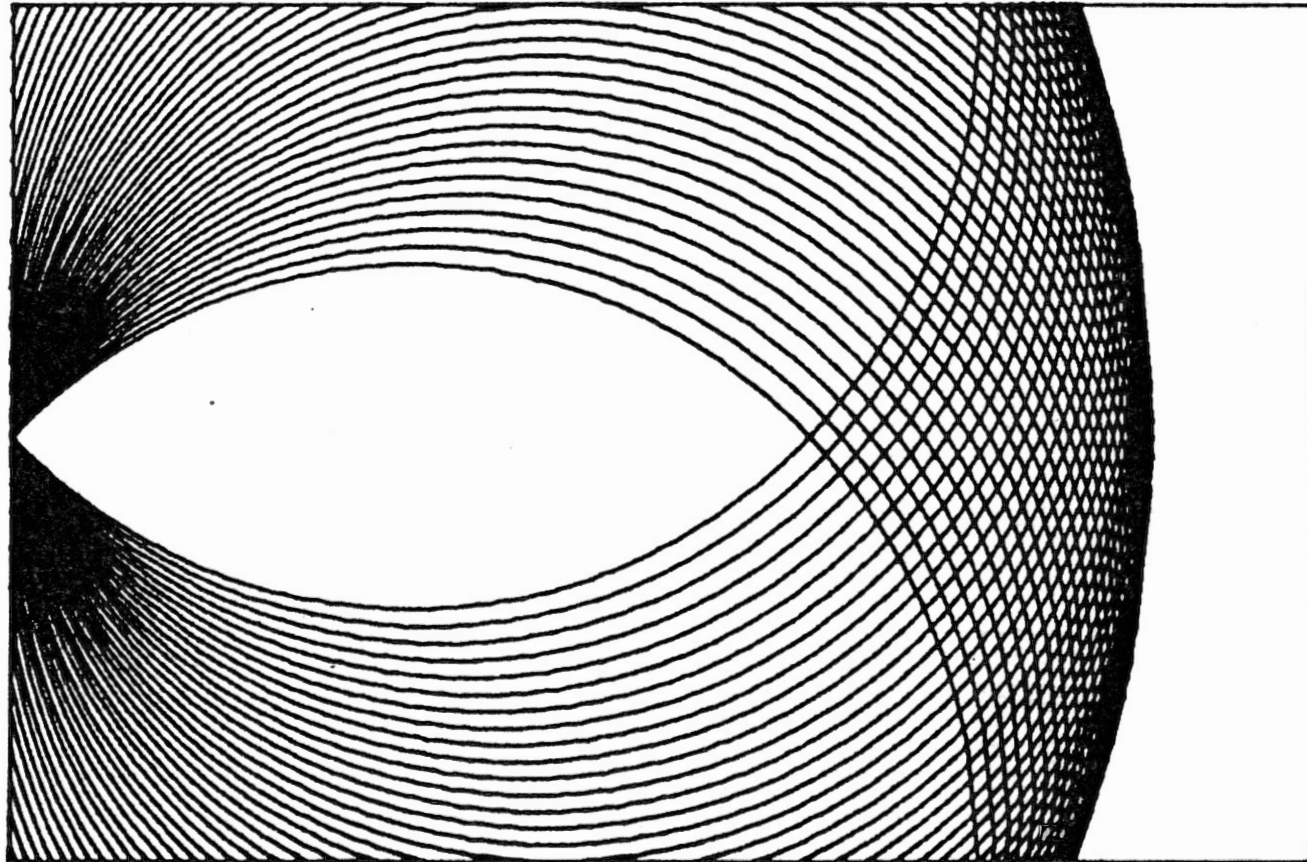


Figure 9. Workarea of a Constrained 3R Robot, $a_2=3.5$, $a_3=3.5$, $S_1=2.5$

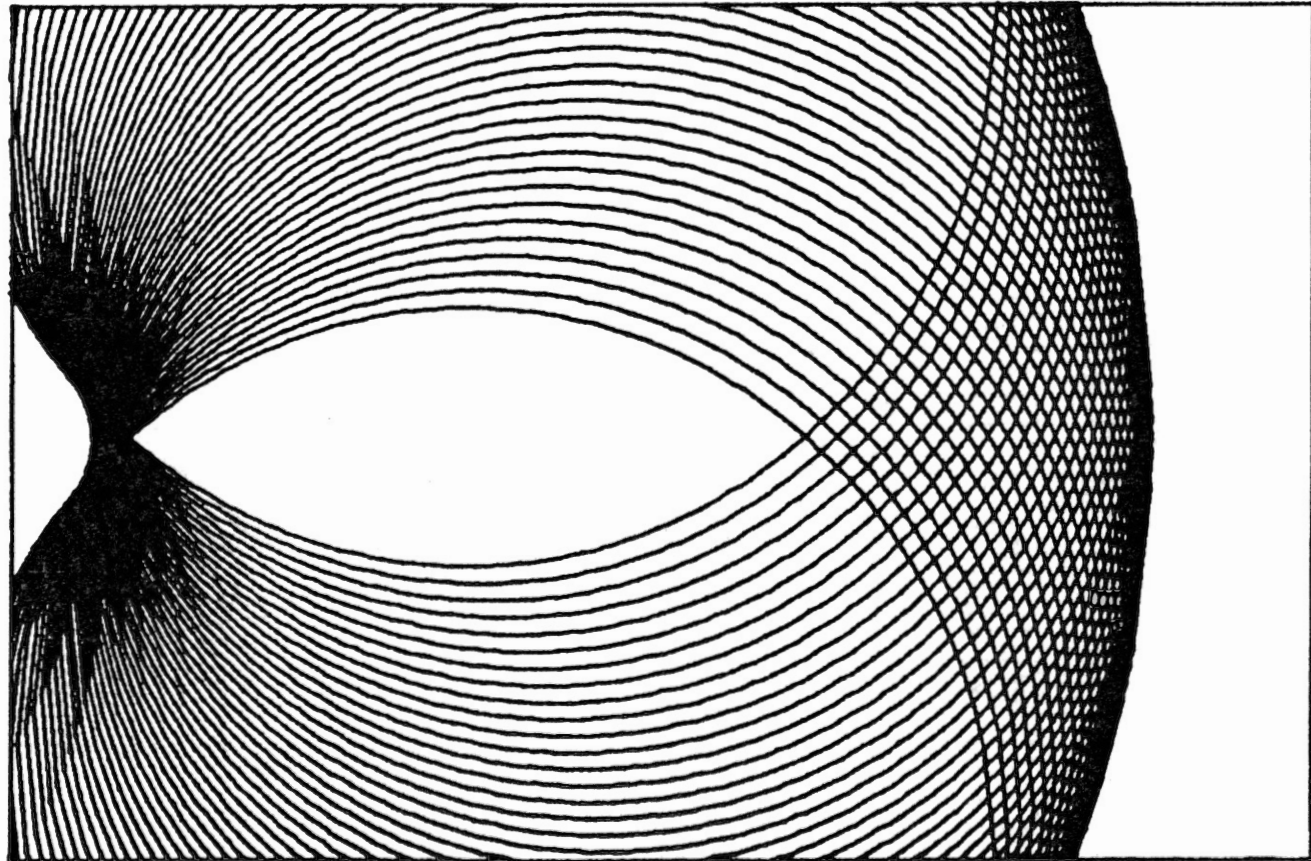


Figure 10. Workarea of a Constrained 3R Robot, $a_2=3.75$, $a_3=3.25$, $s_1=2.5$

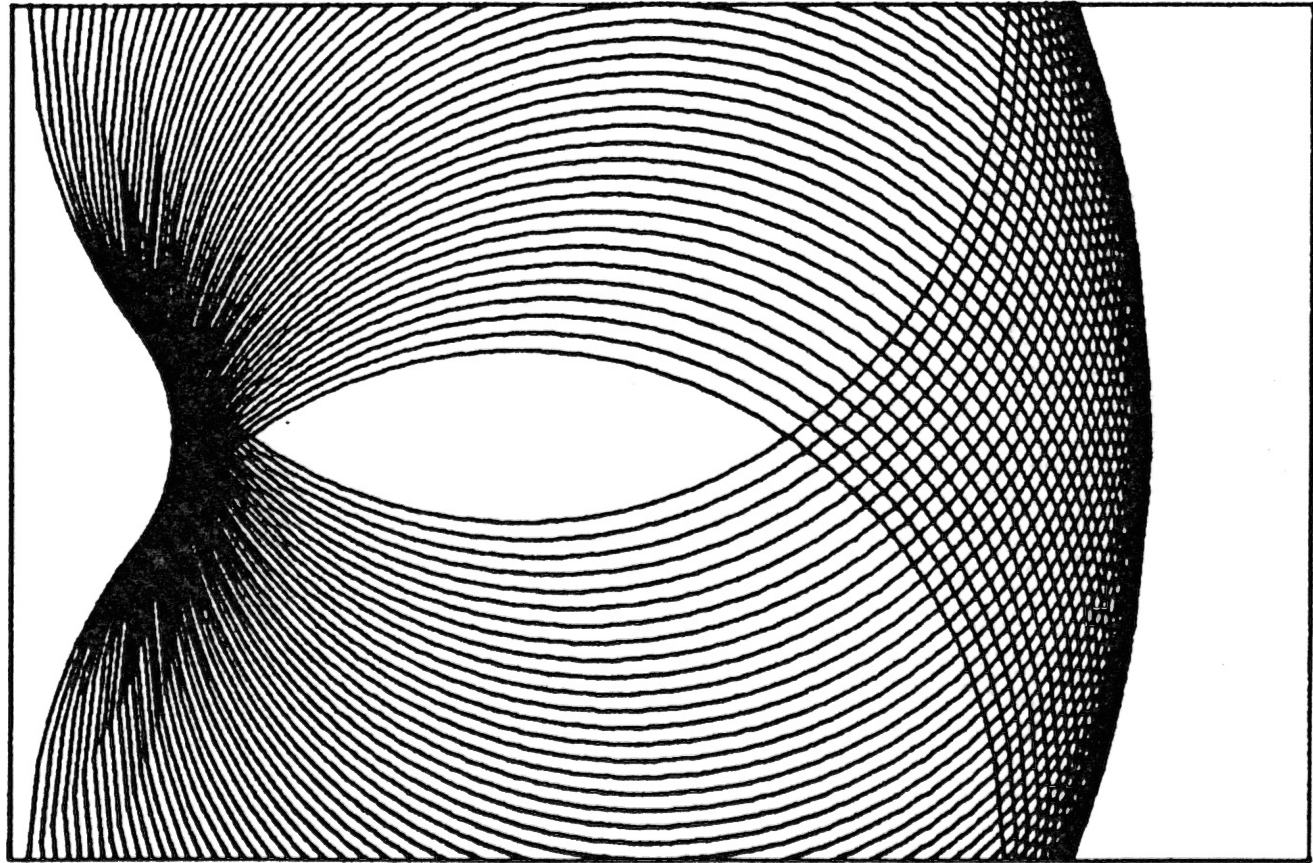


Figure 11. Workarea of a Constrained 3R Robot, $a_2=4.0$, $a_3=3.0$, $S_1=2.5$

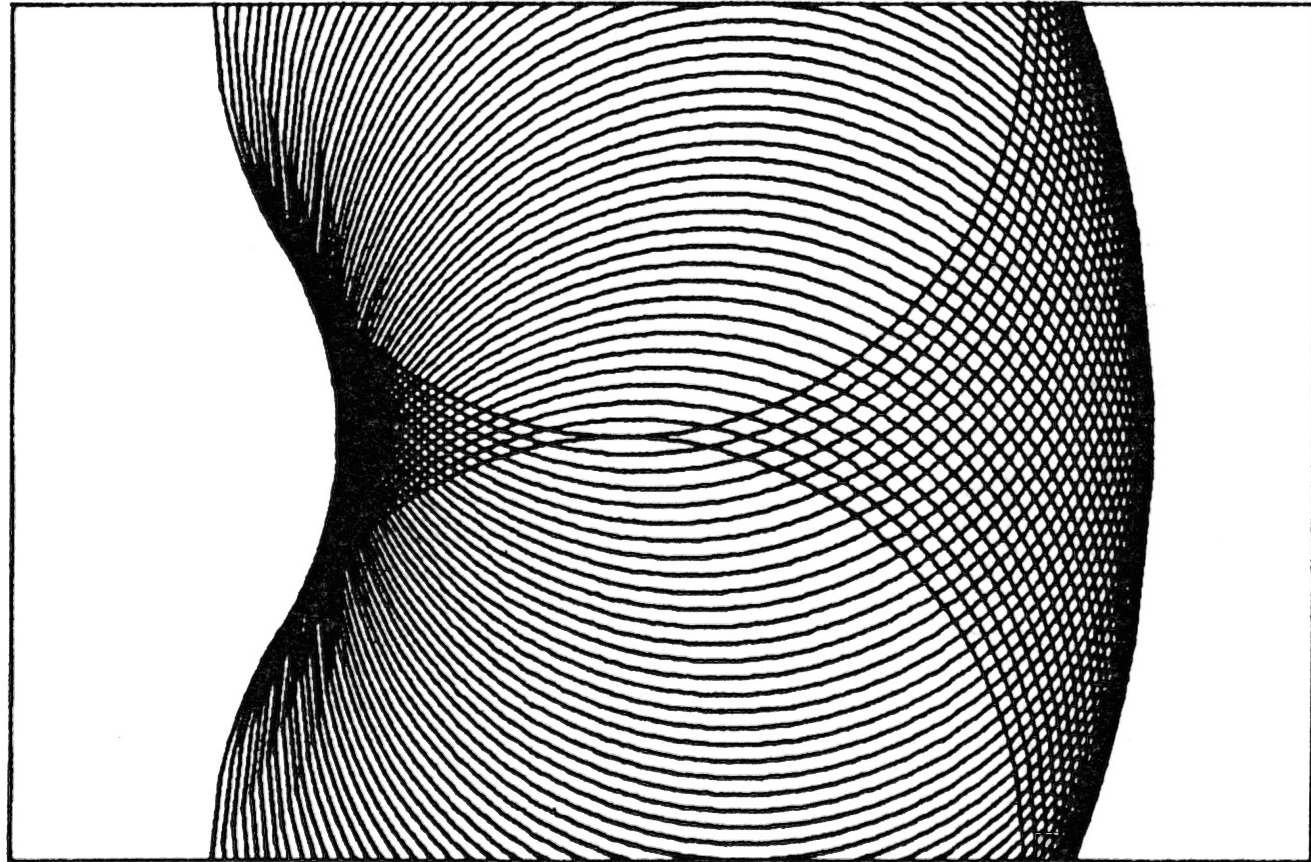


Figure 12. Workarea of a Constrained 3R Robot, $a_2=4.5$, $a_3=2.5$, $S_1=2.5$

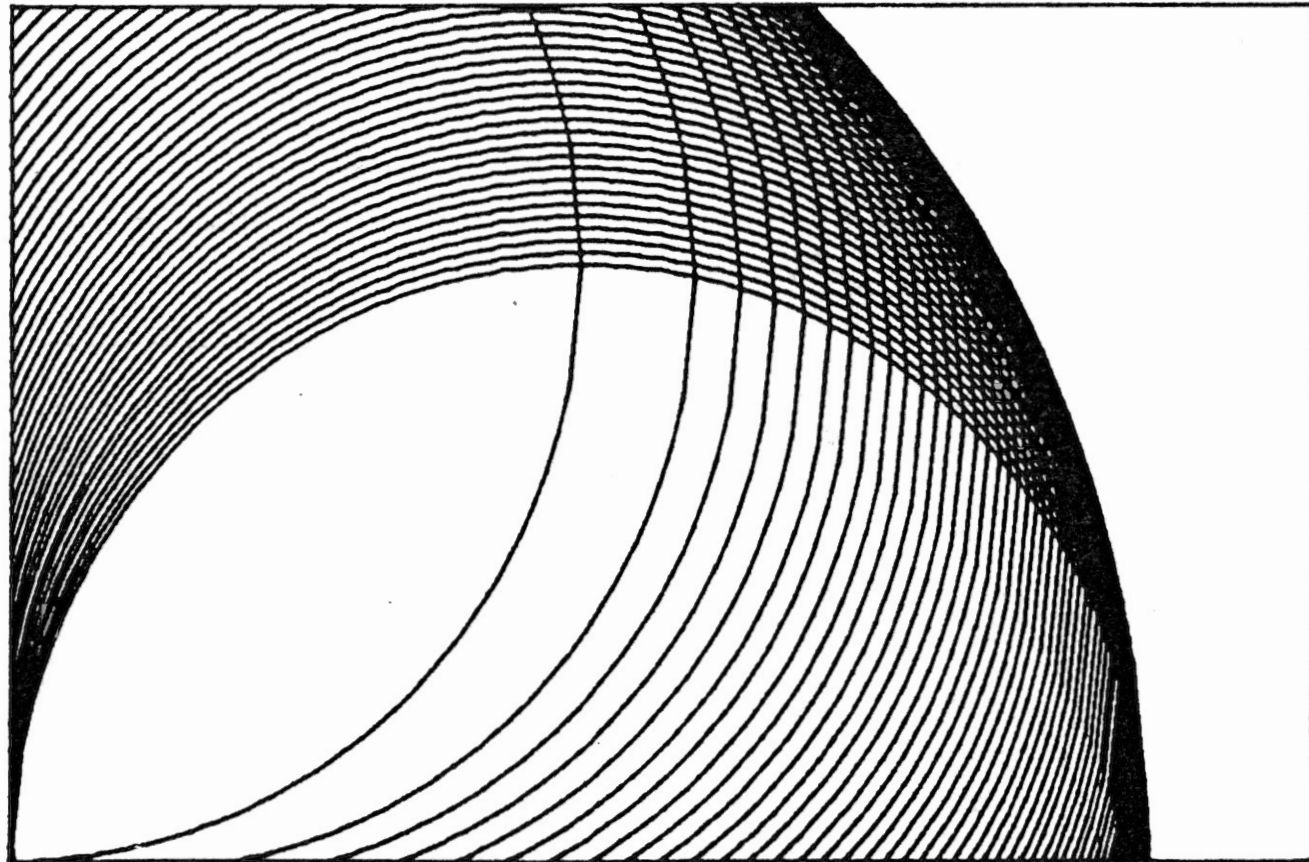


Figure 13. Workarea of a Constrained 3R Robot, $a_2=3.5$, $a_3=3.5$, $S_1=0$

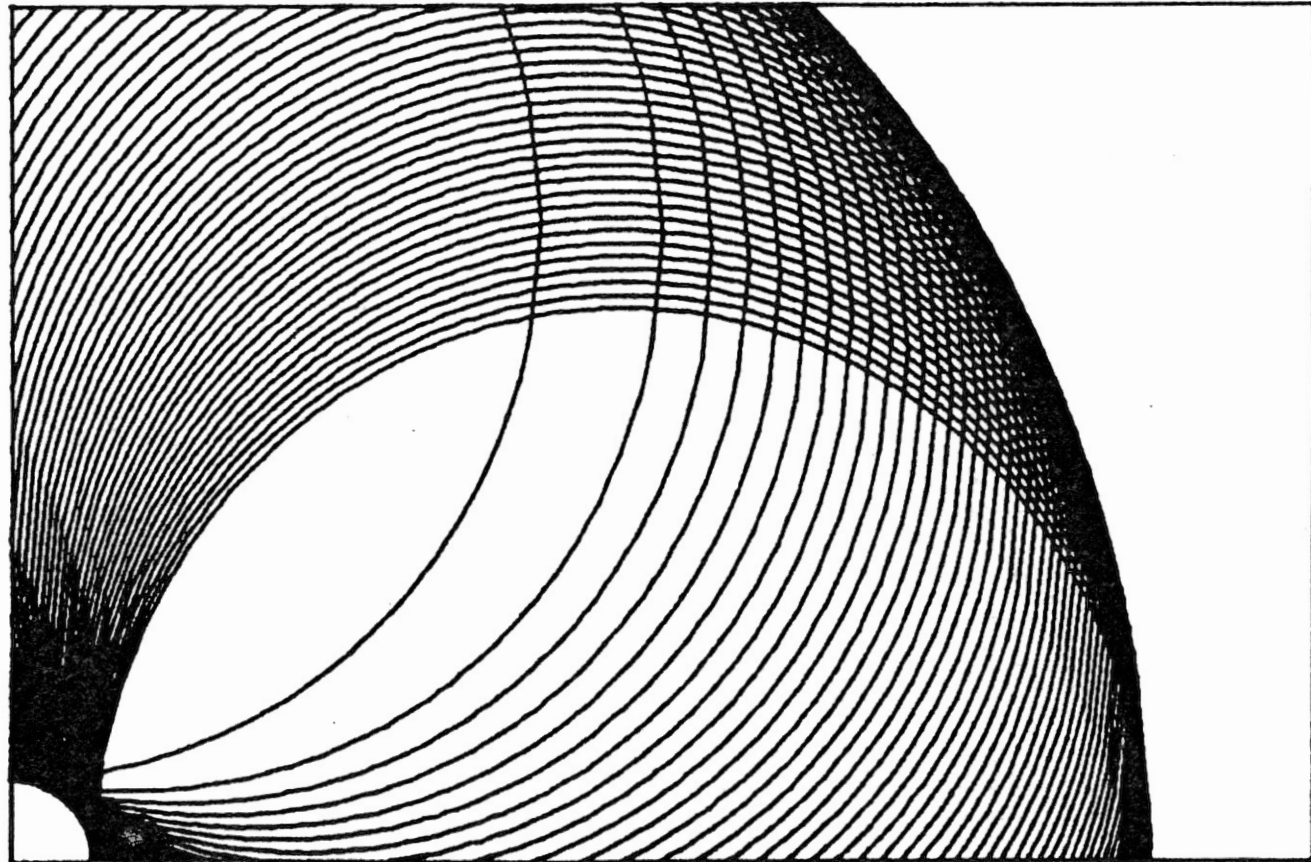


Figure 14. Workarea of a Constrained 3R Robot, $a_2=3.75$, $a_3=3.25$, $s_1=0$

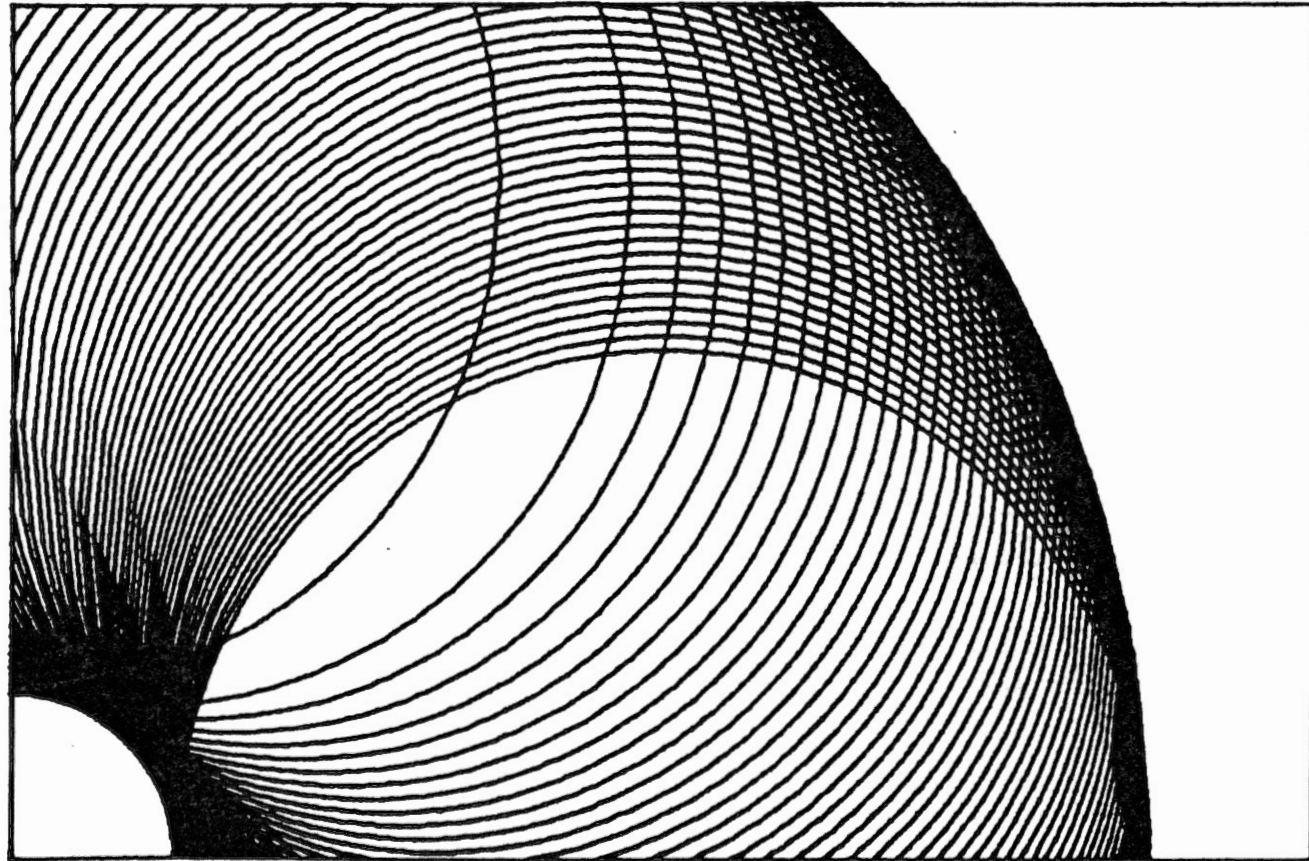


Figure 15. Workarea of a Constrained 3R Robot, $a_2=4.0$, $a_3=3.0$, $S_1=0$

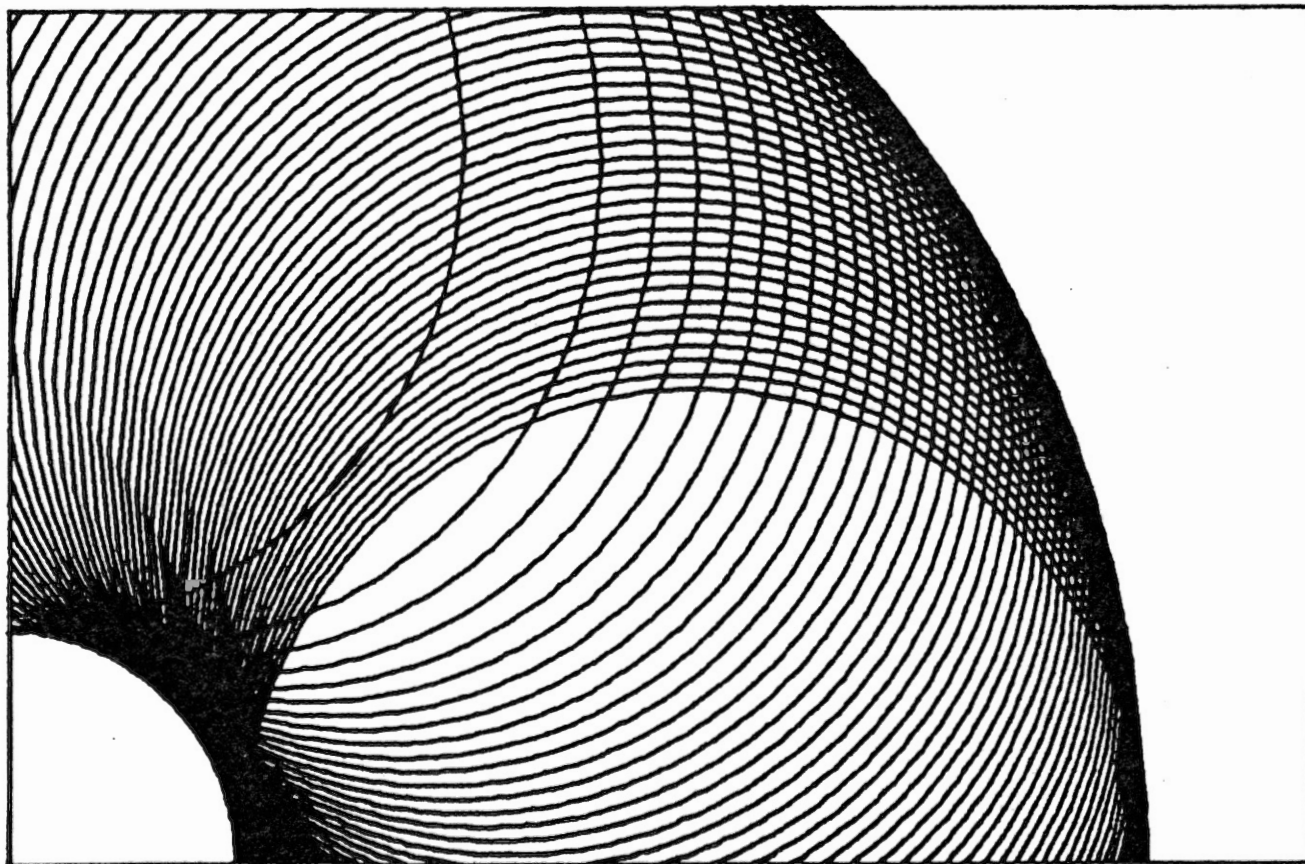


Figure 16. Workarea of a Constrained 3R Robot, $a_2=4.2$, $a_3=2.8$, $S_1=0$

Figures 14 and 15 show the effect of increasing the linklength a_3 and it can be seen that the void within the workarea is reduced by increasing a_3 until in Figure 16 the internal void has disappeared. Therefore, the 'popular' 3R robot with zero offset like in the previous case (Figure 9), will not provide the optimum workarea when space constraints are present.

Figure 17 shows the workarea of a 3R robot ($S_1 = 2.5$, $a_2 = a_3 = 4.19$) when the robot hand in its extended position can reach the right corners of the constrained area. As can be seen from this figure, the large void within the workarea makes this configuration of the robot arm completely unpractical. Figure 18 shows the workarea for $a_2 = 5.88$ and $a_3 = 2.5$. Since $a_3 = h/2$, the void has vanished. The workarea of the robot arm still can be increased by eliminating the offset S_1 from the configuration of the robot arm. Figure 19 shows the workarea of the 3R robot arm with $S_1 = 0$, $a_2 = 5.38$ and $a_3 = 3.0$. The robot arm in Figure 19 can reach one right corner of the constrained workarea, but provides more workarea compared to the robot in Figure 18.

From the results of Chapter II, a 4R robot with link parameters $a_1 = 0$, $a_2 = 2a_3 = 2a_4$, $\alpha_1 = 90^\circ$, $\alpha_2 = \alpha_3 = \alpha_4 = 0$, $S_1 = S_2 = S_3 = S_4 = 0$, was seen to give the best performance regarding the workspace. Figure 20 shows the workarea of the mentioned 4R robot with total link length of seven and the same constraints as the 3R robots in Figures 9 through 19. It can be seen that this robot has a continuous workarea within the constraints and to the extreme reach of the robot hand. Comparing Figure 20 with the 3R cases presented in Figures 8 through

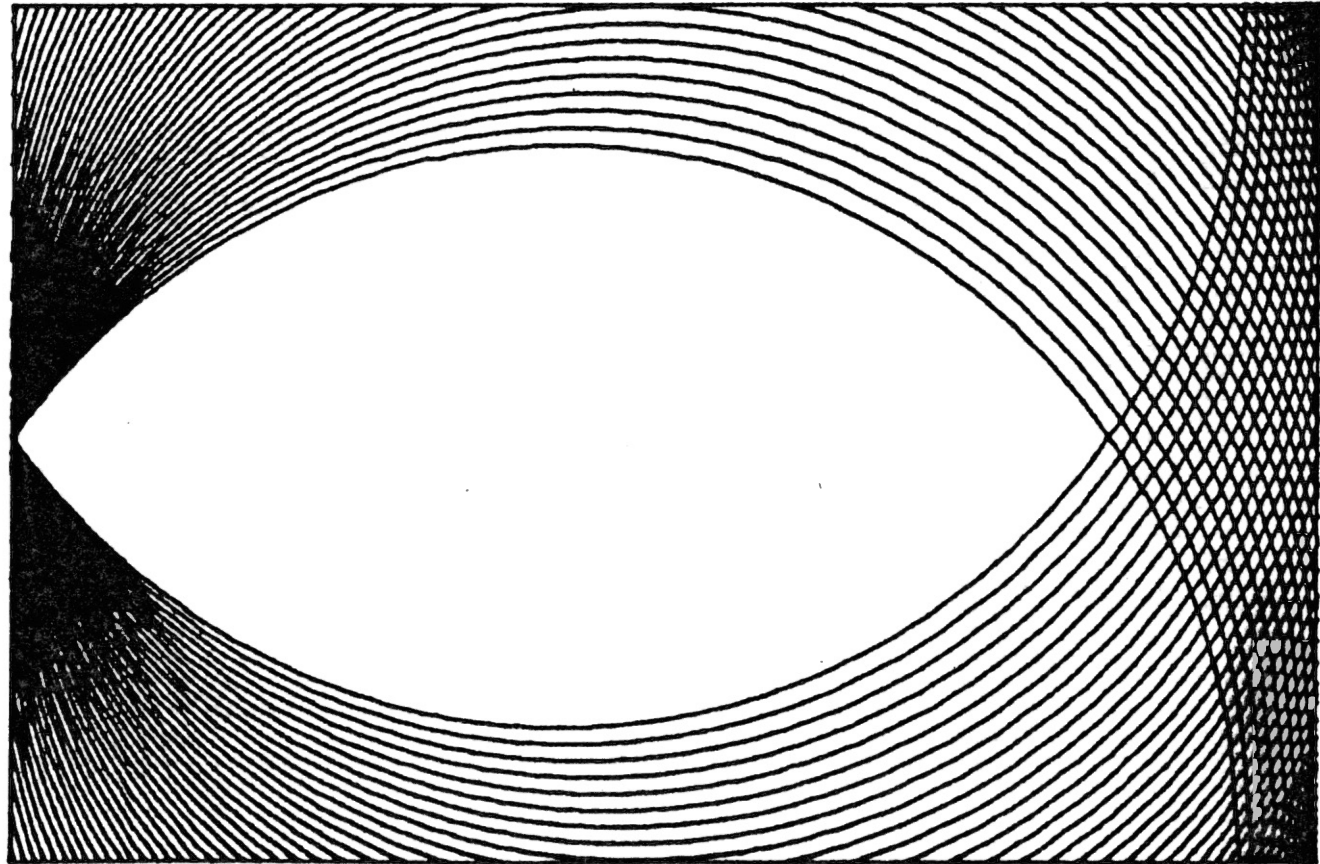


Figure 17. Workarea of a Constrained 3R Robot, $a_2=4.19$, $a_3=4.19$, $S_1=2.5$

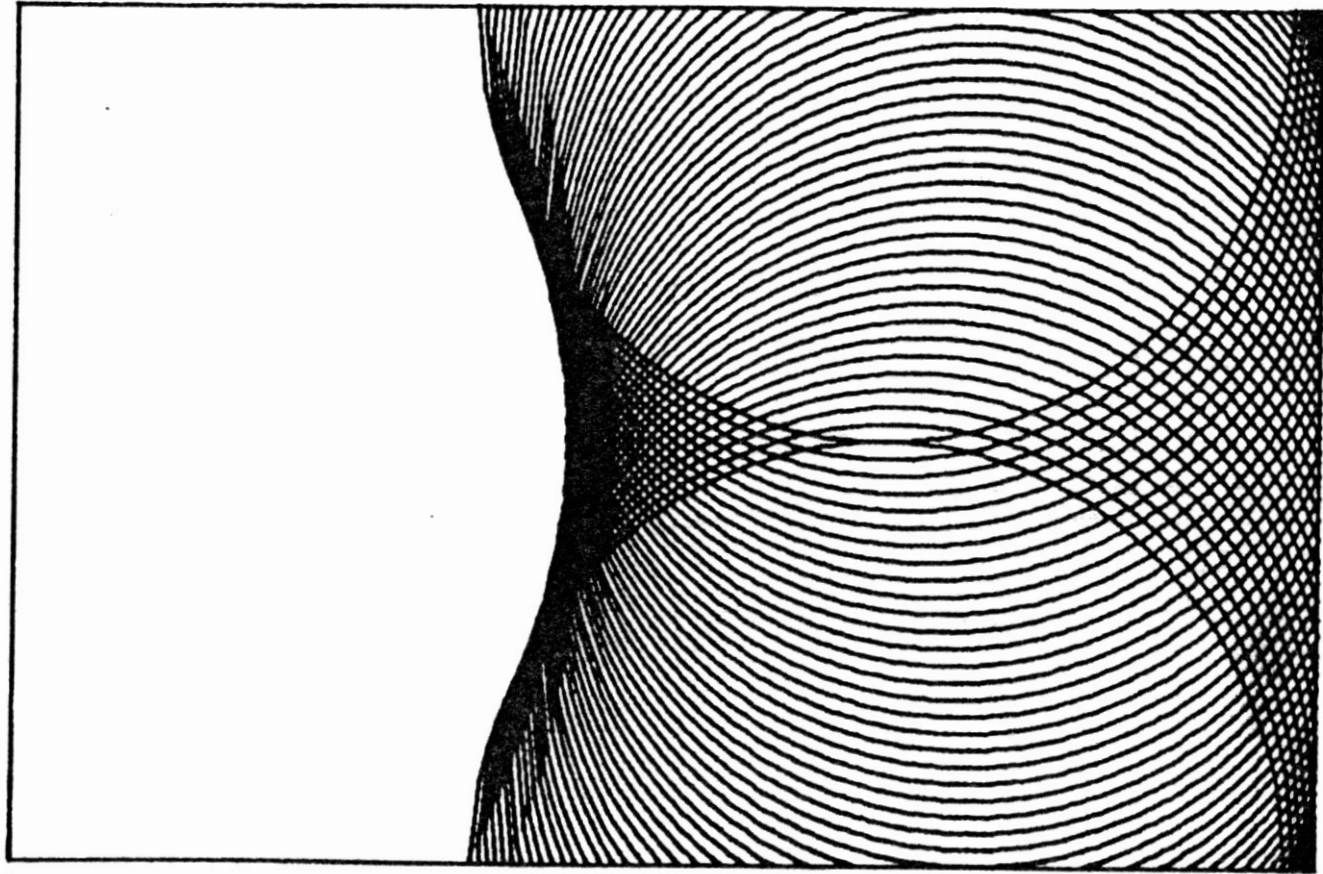


Figure 18. Workarea of a Constrained 3R Robot, $a_2=5.88$, $a_3=2.5$, $S_1=2.5$

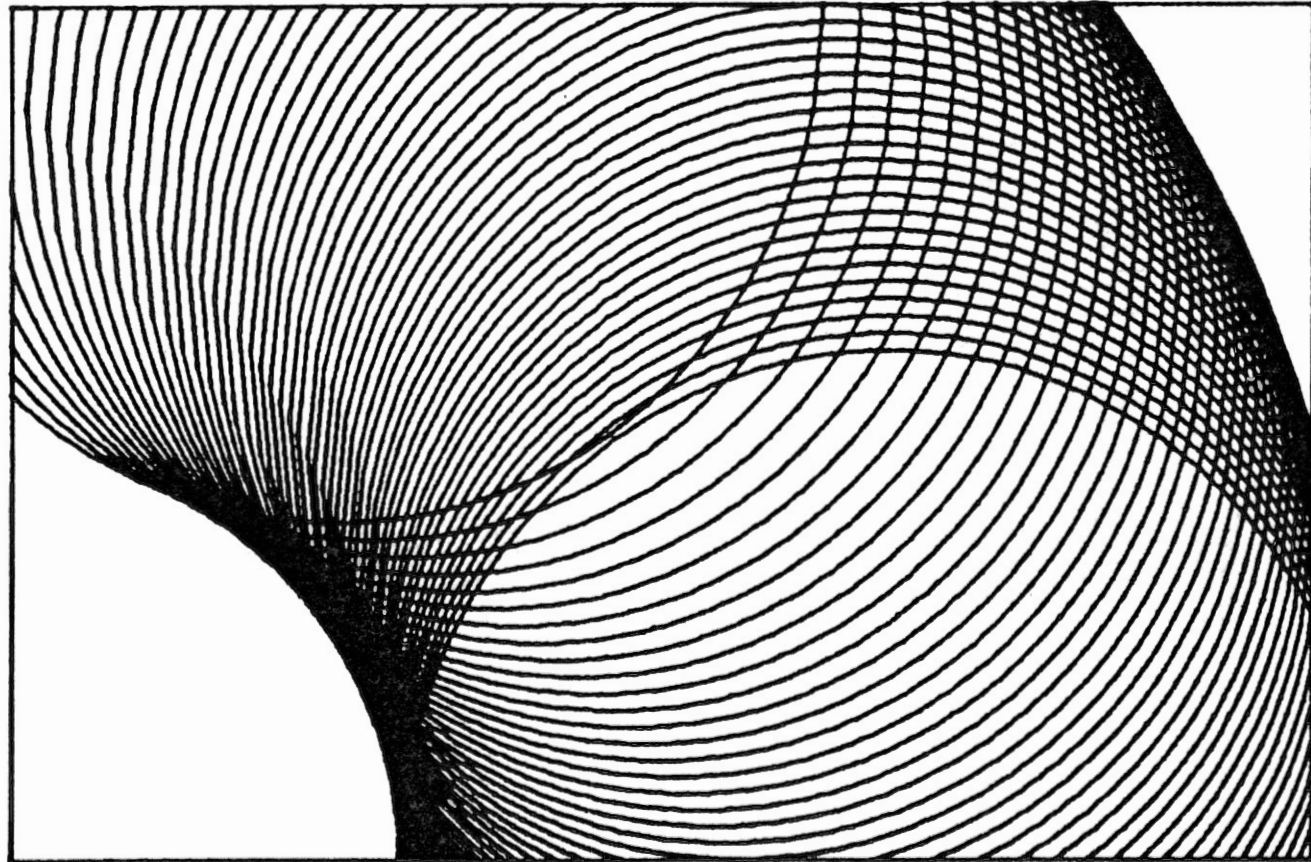


Figure 19. Workarea of a Constrained 3R Robot, $a_2=5.38$, $a_3=3.0$, $S_1=2.5$

Shaded area is the accessible
workarea of 4R robot

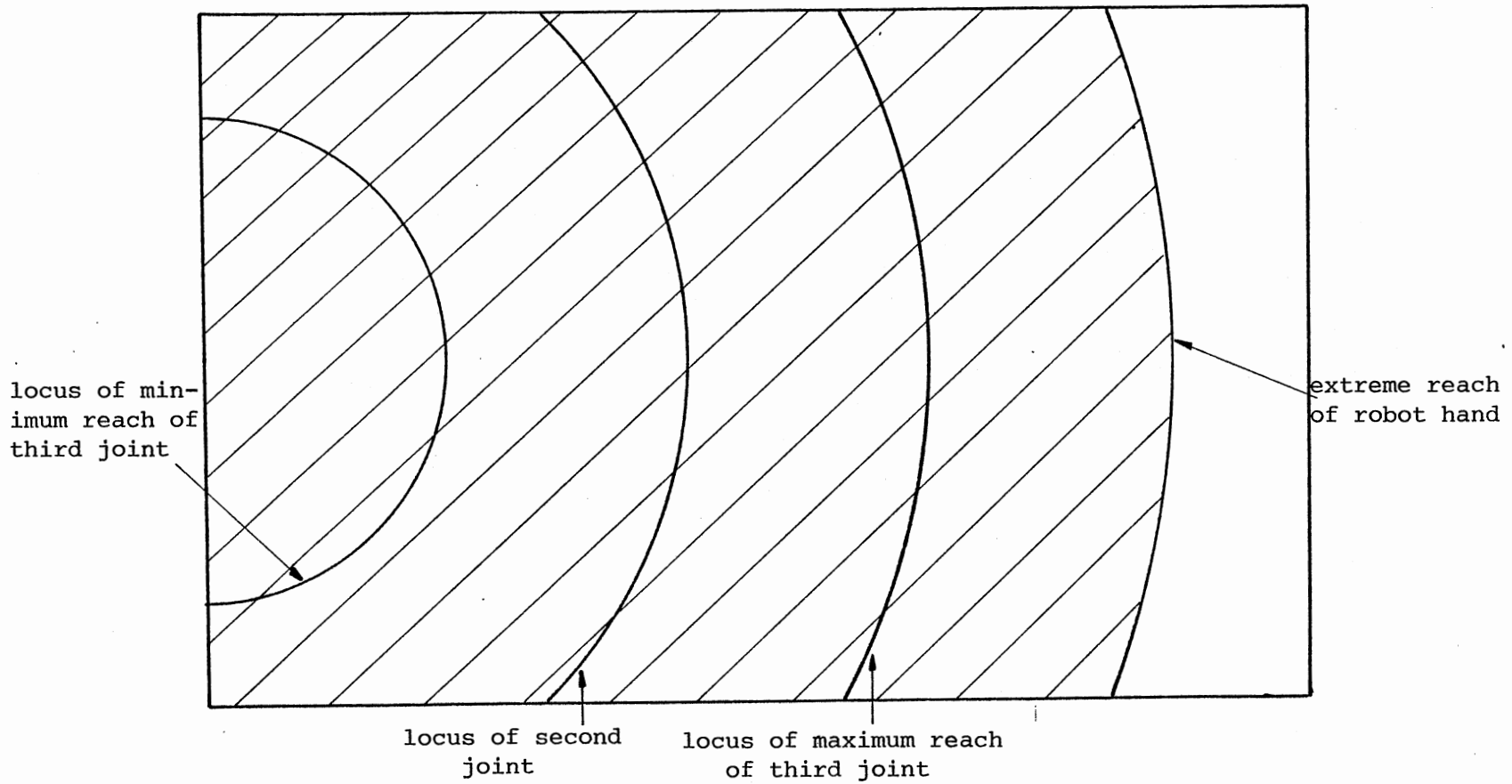


Figure 20. Workarea of a Constrained 4R Robot Arm

12, it is seen that the 4R robot has much better performance in terms of workspace. In addition to having the maximum possible workarea, the 4R robot arm is more capable of reaching a point with more than one configuration of the arm. This capability gives the 4R robot more ability to avoid obstacles.

CHAPTER V

SUMMARY AND RECOMMENDATIONS

5.1 Summary

In this study, several aspects of the performance of 3R and 4R robots have been analyzed. The workspace of a number of 4R configurations has been presented and compared to the 'best' 3R robot. A brief comparison of 3R and 4R joint displacements was done and a computer program for joint displacement analysis based on the iterative velocity method was presented. This study also included a comparison of the effects of space constraints on the workspace of 3R and 4R robot arms.

The study presented in Chapter II revealed that the 4R robot with linkparameters $a_1 = 0$, $a_2 = 2a_3 = 2a_4$, $S_1 = S_2 = S_3 = S_4$, $\alpha_1 = 90^\circ$ and $\alpha_2 = \alpha_3 = \alpha_4 = 0$ represents the best configuration of link parameters. It was seen that although 4R robot arms are more flexible than 3R, not all 4R configurations will have the maximum workspace obtainable with the 'popular' 3R robot arm.

The comparison of 3R and 4R joint displacements presented in Chapter III indicated that the sum of joint displacements for a 4R robot in moving between two stations will in general be larger than for a 3R robot arm. However, in some cases displacements of first and second joints may be smaller for 4R robots, which can mean less energy

consumption. Joint displacements of each robot configuration depend highly on the location of initial and final position of the robot hand.

The iterative velocity method for joint displacement analysis was used effectively for 3R, 4R and 6R robots. This method requires that the robot hand be defined as a rigid body. The iterative velocity method requires a large number of iterations if the distance between initial and final positions is large, which makes it more effective for smaller range of motion.

The workspace of 3R robots can be greatly affected by the presence of space constraints. From the results of Chapter IV, it can be seen that the 'popular' 3R robot may not give the best obtainable workspace in the presence of space constraints. The case study in Chapter IV revealed that a 4R robot with the same motion constraints not only can give the maximum obtainable workspace, but also has the ability of avoiding obstacles.

5.2 Recommendations

The iterative velocity method used in Chapter III requires the position vector and two vectors fixed in the robot hand. This requirement is a limitation when the method is being used for robots with less than six degrees of freedom. It is a recommendation of this study that a method be developed which requires only the position vector and one vector fixed in the robot hand as input.

As a continuation of the study presented in Chapter IV, it is recommended that other configurations of constraints and robot arms be

studied. A general method should be developed for analyzing the constrained workspace, keeping the robot arm within the space constraints.

REFERENCES

1. Roth, B., "Performance Evaluation of Manipulators from a Kinematic Viewpoint," Performance Evaluation of Programmable Robots and Manipulators, NBS Special Publication 459, 1976, pp. 39-62.
2. Gupta, K. C. and Roth, B., "Design Consideration for Manipulator Workspace," ASME Paper No. 810330, 1981.
3. Kumar, A. and Waldron, K. J., "The Workspace of a Mechanical Manipulator," ASME Paper No. 80-DET-107, (Presented at ASME 16th Mechanisms Conference, California, September 28 - October 1, 1980.
4. Tsai, Y. C. and Soni, A. H., "Accessible Region and Synthesis of Robot Arms," ASME Paper No. 80-DET-101, (Presented at ASME 16th Mechanisms Conference, California, September 28 - October 1, 1980.
5. Pieper, D. E., "The Kinematics of Manipulators under Computer Control," Stanford Artificial Intelligence Laboratory Memo AIM-72, 1968.
6. Hartenberg, R. S. and Denavit, J., Kinematic Synthesis of Linkages, McGraw-Hill, New York, 1964, Ch. 12.
7. Milenkovic, V., "Computer Synthesis of Continuous Robot Motion," Proceedings 5th World Congress on the Theory of Machines and Mechanisms, Montreal, 1979, Vol. 2, pp. 1332-1335.
8. Tsai, Y. C., "Synthesis of Robots/Manipulators for a Prescribed Working Space." (Unpublished Ph.D. dissertation, Oklahoma State University, 1982.)
9. Roth, B., "Robots," Applied Mechanics Review, Vol. 31, No. 11, 1978, pp. 1511-1519
10. Shimano, B., "The Kinematic Design and Force Control of Computer-Controlled Manipulators," Ph.D. dissertation, Stanford University, 1978.

APPENDIX A

LISTING OF A PROGRAM FOR
WORKSPACE ANALYSIS

```

DIMENSION A(4,4,4),AD1(4,4),AD2(4,4),AD3(4,4),AD4(4,4),
*B(4,4),C(4,4),D(4,4),RES(4),CNE(4),S(4),ALP(4)
*,AA(4),THA(4),IMAGE(1500)
      DATA BCD/'*  ' /
      CALL PLOT1(0,11,3,11,4)
      CALL PLOT2(IMAGE,1.0,-1.0,1.0,-1.0)
      READ(5,100) (CNE(I),I=1,4)
      READ(5,100) (AA(I),I=1,4)
      READ(5,100) (ALP(I),I=1,4)
      READ(5,100) (S(I),I=1,4)
      DTR=3.141593/180.0
100  FCRMAT(4F10.3)
      DO 101 N=1,4
      ALP(N)=ALP(N)*DTR
101  CCNTINUE
      THA(1)=0.0
      DO 11 I2=1,361,18
      N2=I2-1
      THA(2)=N2*DTR
      DO 11 I3=1,361,18
      N3=I3-1
      THA(3)=N3*DTR
      DO 11 I4=1,361,18
      N4=I4-1
      THA(4)=N4*DTR
      DO 1 I=1,4
      A(I,1,1)=COS(THA(I))
      A(I,1,2)=-SIN(THA(I))*COS(ALP(I))
      A(I,1,3)=SIN(THA(I))*SIN(ALP(I))
      A(I,1,4)=AA(I)*COS(THA(I))
      A(I,2,1)=SIN(THA(I))
      A(I,2,2)=COS(THA(I))*COS(ALP(I))
      A(I,2,3)=-COS(THA(I))*SIN(ALP(I))
      A(I,2,4)=AA(I)*SIN(THA(I))
      A(I,3,1)=0.0
      A(I,3,2)=SIN(ALP(I))
      A(I,3,3)=COS(ALP(I))
      A(I,3,4)=S(I)
      A(I,4,1)=0.0
      A(I,4,2)=0.0
      A(I,4,3)=0.0
      A(I,4,4)=1.0
1    CCNTINUE
      DO 2 I = 1,4
      DO 2 J = 1,4
      AD1(I,J)=A(1,I,J)
      AD2(I,J)=A(2,I,J)
      AD3(I,J)=A(3,I,J)
      AD4(I,J)=A(4,I,J)
2    CONTINUE
      CALL MATMLT(AD1,AD2,B,4,4,4)
      CALL MATMLT(B,AD3,C,4,4,4)
      CALL MATMLT(C,AD4,D,4,4,4)
      CALL MATVEC(D,CNE,RES,4,4)
      PX=0.0
      PY=(RES(1)**2+RES(2)**2)**.5
      PZ=RES(3)
      CALL PLOT3(ECD,PY,PZ,1,4)

```

```

11 CONTINUE
  CALL PLOT4(14,'VERTICAL LABEL')
  WRITE(6,12) (AA(I),I=1,4),(ALP(I),I=1,4),
  *(S(I),I=1,4)
12 FORMAT(1H0,1X,4F10.5)
  STOP
  END

```

```

C ..... T(M,P)=A(M,N)*U(N,P) .....
C

```

```

  SUBROUTINE MATMLT(A,U,T,M,N,P)
  INTEGER P
  DIMENSION A(4,4),T(4,4),U(4,4)
  DO 1 I = 1,M
  DC 1 J = 1,P
  1 T(I,J)=0.0
  DO 2 I=1,M
  DO 2 J=1,P
  DC 2 K=1,N
  2 T(I,J)=A(I,K)*U(K,J)+T(I,J)
  RETURN
  END

```

```

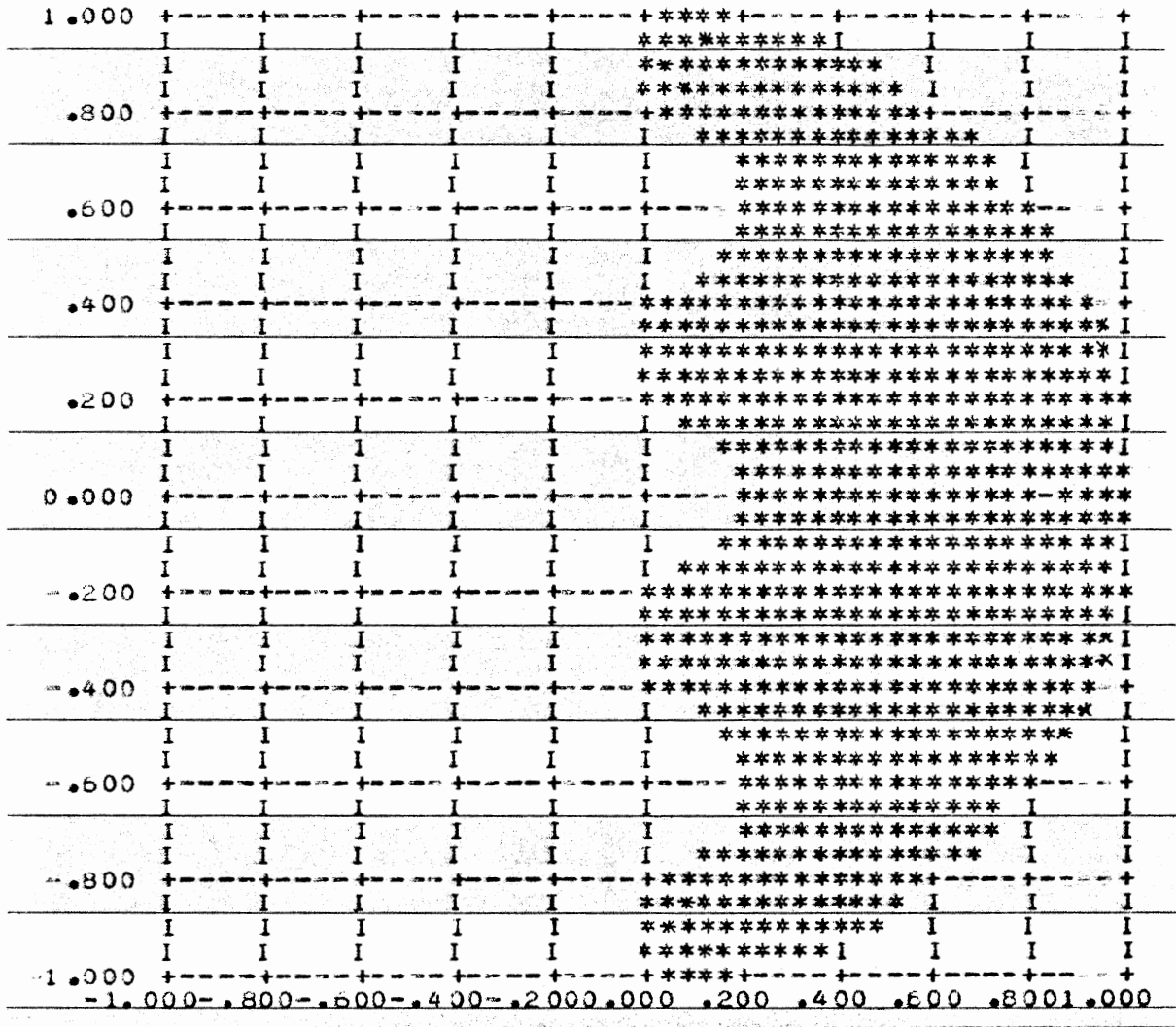
C ..... Z(M)=A(M,N)*X(N) .....
C

```

```

  SUBROUTINE MATVEC(A,X,Z,M,N)
  DIMENSION A(4,4),X(4),Z(4)
  DO 5 I = 1,M
  5 Z(I)=0.0
  DO 6 I = 1,M
  DC 6 J = 1,N
  6 Z(I)=A(I,J)*X(J) + Z(I)
  RETURN
  END

```



$$\alpha_1 = 90^\circ, \alpha_2 = 90^\circ, \alpha_3 = 90^\circ$$

$$a_1 = 0.0, a_2 = 0.6, a_3 = 0.3, a_4 = 0.1$$

$$s_1 = s_2 = s_3 = s_4 = 0.$$

Figure 21. Sample Computer Output Showing the Workarea of a 4R Robot

APPENDIX B

DETAILS OF THE ITERATIVE

VELOCITY METHOD

In section 3.3 the quantities \underline{W} , \underline{n} and ϕ were defined as:

$$\underline{W} = \frac{(\underline{L}_2 - \underline{L}_1) \times (\underline{N}_2 - \underline{N}_1)}{(\underline{L}_2 - \underline{L}_1) \cdot (\underline{N}_2 + \underline{N}_1)} \quad (\text{B.1})$$

$$\underline{n} \tan(\phi/2) = \underline{W} . \quad (\text{B.2})$$

For infinitesimal motion, \underline{W} is related to the angular velocity. In order to find this relation the following procedure can be used:

$$\underline{L}_2 = \underline{L}_1 + \frac{d\underline{L}_1}{dt} (\Delta t) + \frac{d^2\underline{L}_1}{dt^2} (\Delta t)^2 + \dots \quad (\text{B.3})$$

$$\underline{N}_2 = \underline{N}_1 + \frac{d\underline{N}_1}{dt} (\Delta t) + \frac{d^2\underline{N}_1}{dt^2} (\Delta t)^2 + \dots \quad (\text{B.4})$$

$$\phi = \overset{0}{\cancel{\phi}_1} + \frac{d\phi}{dt} (\Delta t) + \frac{d^2\phi}{dt^2} (\Delta t)^2 + \dots \quad (\text{B.5})$$

Using Equations (B.3) and (B.4) in Equation (B.1):

$$\underline{W} = \frac{\frac{d\underline{L}_1}{dt} (\Delta t) + \frac{d\underline{N}_1}{dt} (\Delta t) + \dots}{\frac{d\underline{L}_1}{dt} (\Delta t) \cdot 2\underline{N}_1 + \dots} \quad (\text{B.6})$$

and in its equivalent from Equation (B.2):

$$\underline{W} = \underline{n} \tan\left\{ \frac{\dot{\phi}}{2} (\Delta t) + \dots \right\} . \quad (\text{B.7})$$

Equating the right-hand sides of Equations (B.6) and (B.7) and

simplifying, the following can be obtained:

$$\dot{\phi} \underline{n} = \frac{\frac{dL_1}{dt} \times \frac{dN_1}{dt}}{\frac{dL_1}{dt} \cdot N_1}$$

which is the equivalent expression for the angular velocity of the hand.

The angular velocity \underline{W} can be approximated as

$$\underline{W} = \frac{\Delta\phi}{\Delta t} \underline{n} .$$

The approximate velocity of a point in the hand at the origin is

$$\underline{V} = H \underline{W} - \underline{W} \times \underline{r}$$

or

$$\underline{V} = H \frac{\Delta\phi}{\Delta t} \underline{n} - \frac{\Delta\phi}{\Delta t} \underline{n} \times \underline{r}$$

where H , $\Delta\phi$, \underline{n} and \underline{r} are the screw parameters formed from the change in the hand position and orientation.

APPENDIX C

LISTING OF A PROGRAM FOR JOINT DISPLACEMENT

ANALYSIS USING THE ITERATIVE

VELOCITY METHOD

```

C
C*****
C
C   THIS IS A JOINT DISPLACEMENT ANALYSIS
C   PROGRAM BASED ON THE ITERATIVE VELOCITY
C   METHOD.  IN THIS VERSION, A 6R
C   ROBOT IS ANALYZED.
C
C   DEVELOPED BY ALIREZA BEHBOUD DURING
C   SPRING SEMESTER AT OSU 1982.
C
C*****
C
C   DIMENSION RL1(3),RN1(3),RL2(3),RN2(3),RP1(3),RP2(3),
C   $THA(6),S(6),AA(6),ALP(6),RN(3),RR(3),DV1(3),DV2(3),
C   $DV3(3),PE1(3),PE2(3),PE3(3),AC(6,6),WKAREA(54),BB(6),
C   $DT(6),RJ1(3),XW1(3),XW2(3),XW3(3),XY(3),PE4(3),DV4(3),XW4(3),
C   $PE5(3),PE6(3),DV5(3),DV6(3),XW5(3),XW6(3)
C
C   COMMON /BLOCK1/N,S,AA,ALP,THA,RJ1,DV1,PE1,RL1,RN1,RL2,
C   $RN2,RP1,RP2
C
C   DTR=3.1415927/180.0
C   DO 102 I=1,6
C   ALP(I)=ALP(I)*DTR
C   THA(I)=THA(I)*DTR
102 CONTINUE
C   DATA DEL/4.0/
C   DATA NNNMAX/40/
C   DATA DIFMAX/.001/,THM/4.0/
C   NNN=1
C   DTR=3.1415927/180.0
C   REV=1.0/DTR
C
C   ..... COMPUTE THE SCREW PARAMETERS FROM POSITION 1 TO POSITION 2
C
1   CONTINUE
C   CALL SCRE(RN,RR,PHI,H)
C   WRITE(6,30) (RN(I),I=1,3),(RR(I),I=1,3),PHI,H
30  FORMAT(1H0,1H0,2X,'RN=(',3G15.5,')',2X,'RR=(',3G15.5,')',
C   $/,3X,'PHI=',G15.5,3X,'H=',G15.5)
C   PHI=PHI*REV
C   IF (PHI.LE.DEL) GO TO 2
C
C   ..... SPECIFY INTERMEDIATE GOAL BY DEL/PHI .....
C
C   PHI=DEL/PHI
C   PHI=PHI*DTR
C   GO TO 128
2   CONTINUE
C   PHI=PHI*DTR
128 CONTINUE
C
C   WRITE(6,32) PHI
32  FORMAT(1H0,3X,'PHI=',G15.5)
C
C   ..... USING SUBROUTINE POS FIND R(I) AND N(I) ...
C

```

```

      CALL PJS(DV1,DV2,DV3,DV4,DV5,DV6,PE1,PE2,PE3,PE4,PE5,PE6)
C
      WRITE(6,35) (DV1(I),I=1,3),(DV2(I),I=1,3),(DV3(I),I=1,3),
      $(DV4(I),I=1,3),(DV5(I),I=1,3),(DV6(I),I=1,3)
35   FORMAT(1H0,2X,'DV1=',3G15.5,/,3X,'DV2=',3G15.5,
      $/,3X,'DV3=',3G15.5,/,3X,'DV4=',3G15.5,/,3X,'DV5=',3G15.5,/,
      $3X,'DV6=',3G15.5)
C
      CALL VECRS(DV1,PE1,XW1)
      CALL VECRS(DV2,PE2,XW2)
      CALL VECRS(DV3,PE3,XW3)
      CALL VECRS(DV4,PE4,XW4)
      CALL VECRS(DV5,PE5,XW5)
      CALL VECRS(DV6,PE6,XW6)
      CALL VECRS(RN,RR,XY)
C
      DO 23 I=1,3
      AC(I,1)=DV1(I)
      AC(I,2)=DV2(I)
      AC(I,3)=DV3(I)
      BB(I)=PHI*RN(I)
23   CONTINUE
C
      DO 129 I=1,3
      J=I+3
      AC(J,1)=XW1(I)
      AC(J,2)=XW2(I)
      AC(J,3)=XW3(I)
129  CONTINUE
C
      DO 130 I=1,3
      AC(I,4)=DV4(I)
      AC(I,5)=DV5(I)
      AC(I,6)=DV6(I)
130  CONTINUE
C
      DO 131 I=1,3
      J=I+3
      AC(J,4)=XW4(I)
      AC(J,5)=XW5(I)
      AC(J,6)=XW6(I)
131  CONTINUE
C
      DO 132 I=1,3
      J=I+3
      BB(J)=PHI*XY(I)-H*PHI*RN(I)
132  CONTINUE
C
C ..... USING IMSL ROUTINES FIND DT(I) VALUES. ....
C
      IN=6
      IM=1
      IA=6
      IDGT=3
C
      CALL LEQT2F(AC,IM,IN,IA,BB,IDGT,WKAREA,IER)
C
      DO 4 I=1,6
      DT(I)=BB(I)
4    CONTINUE

```

```

C
WRITE(6,40) (DT(I),I=1,6)
40 FORMAT(1H0,3X,'DT=(',6G14.5,')')
C
DTMAX=-1.E75
DO 5 I=1,6
DTMAX=AMAX1(DT(I),DTMAX)
5 CONTINUE
C
WRITE(6,50) DTMAX
50 FORMAT(1H0,2X,'DTMAX=',G15.5)
DTMAX=DTMAX*REV
IF (DTMAX.LE.THM) GO TO 7
CH=THM/DTMAX
CH=CH*DTR
DO 6 I=1,6
DT(I)=DT(I)-CH
6 CONTINUE
7 CONTINUE
C
WRITE(6,55) (DT(I),I=1,6)
55 FORMAT(1H0,2X,'DT=(',6G15.5,')')
C
C ..... COMPUTE NEW POSITION 1 BASED ON THESE ANGLE CHANGES ...
C
DO 8 I=1,6
THA(I)=THA(I)+DT(I)
8 CONTINUE
C
WRITE(6,60) (THA(I),I=1,6)
60 FORMAT(1H0,2X,'THA=(',6G15.5,')')
C
CALL ENDP(RP1,RL1,RN1)
C
WRITE(6,65) (RP1(I),I=1,3),(RL1(I),I=1,3),(RN1(I),I=1,3)
65 FORMAT(1H0,3X,'RP1=',3G15.5,/,3X,'RL1=',3G15.5,/,
3X,'RN1=',3G15.5)
C
C ..... CHEK TO SEE IF NEW RP1 IS CLOSE TO RP2. ...
C
DIF1=RP2(1)-RP1(1)
DIF2=RP2(2)-RP1(2)
DIF3=RP2(3)-RP1(3)
DIFM=AMAX1(ABS(DIF1),ABS(DIF2),ABS(DIF3))
IF (DIFM.LE.DIFMAX) GO TO 9
C
C ..... CHEK FOR THE MAXIMUM NUMBER OF ITERATIONS (NNNMAX). ...
C
IF (NNN.GT.NNNMAX) GO TO 9
NNN=NNN+1
GO TO 1
9 CONTINUE
C
WRITE(6,31) IER
31 FORMAT(1H0,3X,I10)
WRITE(6,11) (THA(I),I=1,6)
11 FORMAT(1H0,2X,6G15.5)
WRITE(6,12) NNN
12 FORMAT(1H0,/,3X,I10)
WRITE(6,13) (RP1(I),I=1,3),(RP2(I),I=1,3)

```

```

13  FORMAT(1H0,3X,3G16.5,/,3X,3G15.5)
      STOP
      END

C
C ..... DEFINING INPUT DATA .....
C

      BLOCK DATA
      COMMON /BLOCK1/N,S,AA,ALP,THA,RJ1,DV1,PE1,RL1,RN1,RL2,
$RN2,RP1,RP2
      REAL S(6)/0.0,0.0,0.0,0.0,0.0,0.0/
      REAL AA(6)/0.0,2.0,2.0,1.0,0.5,0.3/
      REAL ALP(6)/90.0,0.0,-90.0,90.0,-90.0,0.0/
      REAL THA(6)/60.0,40.0,30.0,20.0,50.0,70.0/
      REAL RJ1(3)/0.0,0.0,0.0/
      REAL DV1(3)/0.0,0.0,1.0/
      REAL PE1(3)/0.0,0.0,0.0/
      REAL RL1(3)/-.97257,.23188,-.018272/
      REAL RN1(3)/-.19821,.86732,.45659/
      REAL RL2(3)/-.68807,.38511,-.61502/
      REAL RN2(3)/-.051735,-.87143,-.48779/
      REAL RP1(3)/.45728,2.2708,4.4573/
      REAL RP2(3)/-.25300,1.6519,4.4433/
      INTEGER N/6/
      END

C
C ..... SUBROUTINES .....
C
C*****
C   THIS SUBROUTINE FINDS THE POSITION OF THE
C   ROBOT HAND AND THE DIRECTION OF TWO UNIT
C   VECTORS FIXED IN THE HAND
C*****
C

      SUBROUTINE ENDP(RRP1,RRL1,RRN1)
      DIMENSION A(6,4,4),AD1(4,4),AD2(4,4),AD3(4,4),AD4(4,4),
$B(4,4),C(4,4),D(4,4),ALP(6),S(6),AA(6),THA(6),RL1(3),
$RN1(3),RL2(3),RRP1(3),RRL1(3),RRN1(3),
$RJ1(3),DV1(3),PE1(3),RN2(3),RP1(3),RP2(3),AD5(4,4),AD6(4,4)
$,F(4,4),E(4,4)
      COMMON /BLOCK1/N,S,AA,ALP,THA,RJ1,DV1,PE1,RL1,RN1,RL2,
$RN2,RP1,RP2

C
      DO 1 I=1,N
      A(I,1,1)=COS(THA(I))
      A(I,1,2)=-SIN(THA(I))*COS(ALP(I))
      A(I,1,3)=SIN(THA(I))*SIN(ALP(I))
      A(I,1,4)=AA(I)*COS(THA(I))
      A(I,2,1)=SIN(THA(I))
      A(I,2,2)=COS(THA(I))*COS(ALP(I))
      A(I,2,3)=-COS(THA(I))*SIN(ALP(I))
      A(I,2,4)=AA(I)*SIN(THA(I))
      A(I,3,1)=0.0
      A(I,3,2)=SIN(ALP(I))
      A(I,3,3)=COS(ALP(I))
      A(I,3,4)=S(I)
      A(I,4,1)=0.0

```

```

      A(I,4,2)=0.0
      A(I,4,3)=0.0
      A(I,4,4)=1.0
1     CONTINUE
      DO 2 I=1,4
      DO 2 J=1,4
      AD1(I,J)=A(1,I,J)
      AD2(I,J)=A(2,I,J)
      AD3(I,J)=A(3,I,J)
      AD4(I,J)=A(4,I,J)
      AD5(I,J)=A(5,I,J)
      AD6(I,J)=A(6,I,J)
2     CONTINUE
      CALL MATMLT(AD1,AD2,B,4,4,4)
      CALL MATMLT(B,AD3,C,4,4,4)
      CALL MATMLT(C,AD4,D,4,4,4)
      CALL MATMLT(D,AD5,E,4,4,4)
      CALL MATMLT(E,AD6,F,4,4,4)
      DO 6 I=1,3
      RRP1(I)=F(I,4)
      RRL1(I)=F(I,1)
      RRN1(I)=F(I,3)
6     CONTINUE
      RETURN
      END
C
C*****
C
C     SUBROUTINE SCRE FINDS THE SCREW MOTION PARAMETERS
C
C*****
      SUBROUTINE SCRE(RN,RR,PHI,H)
      DIMENSION RL1(3),RN1(3),RL2(3),RN2(3),RP1(3),RP2(3),W(3),
      $RLSUB(3),RNSUB(3),RNSUM(3),RNUM(3),RN(3),RPSUM(3),RPSUB(3),
      $VEC1(3),VEC2(3),VEC3(3),VEC4(3),VEC5(3),VEC6(3),RR(3),
      $S(6),AA(6),ALP(6),THA(6),RJ1(3),DV1(3),PE1(3)
      COMMON /BLOCK1/N,S,AA,ALP,THA,RJ1,DV1,PE1,RL1,RN1,RL2,
      $RN2,RP1,RP2
C
      CALL VECSUB(RL2,RL1,RLSUB,3)
      CALL VECSUB(RN2,RN1,RNSUB,3)
      CALL VECSUM(RN2,RN1,RNSUM,3)
      CALL VECRS(RLSUB,RNSUB,RNUM)
      CALL VECVEC(RLSUB,RNSUM,DEN,3)
      SD=1./DEN
C
C.....CALCULATE W .....
C
      CALL SCAVEC(SD,RNUM,W,3)
      CALL VECLEN(W,WL,3)
      RWL=1./WL
C
C..... CALCULATE RN=N
C
      CALL SCAVEC(RWL,W,RN,3)
      PHI=2.*ATAN(WL)
C
C.....FIND THE SUMATION OF RPSUM=P1+P2 .....
C

```



```

      CALL VEC SUM(RP1,RP2,RPSUM,3)
C
C.....FIND THE RPSUB =P2-P1 .....
C
      CALL VEC SUB(RP2,RP1,RPSUB,3)
C
C.....FIND W**2=WSQR .....
C
      CALL VEC VEC(W,W,WSQR,3)
C.....FIND RMSQR=1.0/WSQR .....
      RMSQR=1.0/WSQR
      CALL SCA VEC(RMSQR,RPSUB,VEC1,3)
      CALL SCA VEC(RMSQR,RPSUM,VEC2,3)
      CALL VEC VEC(W,VEC2,RNUM1,3)
      CALL SCA VEC(RNUM1,W,VEC3,3)
      CALL VEC RS(W,VEC1,VEC4)
      CALL VEC SUB(VEC4,VEC3,VEC5,3)
      CALL VEC SUM(RPSUM,VEC5,VEC6,3)
C
C.....FIND THE VECTOR R=RR
C
      CALL SCA VEC(.5,VEC6,RR,3)
C..... CALCULATE THE MAGNITUDE OF TRANSLATIONS
      CALL VEC VEC(W,RPSUB,RNUM6,3)
C..... CALCULATE THE MAGNITUDE OF THE TRANSLATION S ...
      SS = RNUM6/WL
C..... FIND PITCH OF SCREW ....
      H =ABS(SS/PHI)
      RETURN
      END
C
C*****
C
C      SUBROUTINE POS FINDS THE ORIENTATION OF THE JOINT
C      AXES, FINDS VECTORS PERPENDICULAR TO THE JOINT AXES
C
C*****
C
      SUBROUTINE POS(DDV1,DV2,DV3,DV4,DV5,DV6,PPE1,PE2,PE3,PE4,PE5,PE6)
      COMMON /BLOCK1/N,S,AA,ALP,THA,RJ1,DV1,PE1,RL1,RN1,RL2,
      $RN2,RP1,RP2
      DIMENSION A(6,4,4),AD1(4,4),AD2(4,4),AD3(4,4),AD4(4,4),
      $B(4,4),C(4,4),D(4,4),RES(4),RES1(4),ONE(4),S(6),ALP(6),
      $AA(6),THA(6),RJ1(3),RJ2(3),RJ3(3),RJ4(3),CV1(3),DV2(3),DV3(3),
      $DV4(3),PE1(3),PE2(3),PE3(3),PE4(3),VL2(3),VL3(3),VL4(3),
      $RL1(3),RN1(3),RL2(3),RN2(3),RP1(3),RP2(3),DDV1(3),PPE1(3),
      $AD5(4,4),AD6(4,4),E(4,4),F(4,4),PE5(3),PE6(3),VL5(3),VL6(3)
      $,DV5(3),DV6(3),RJ5(3),RJ6(3)
C
      DO 23 I=1,3
      DDV1(I)=DV1(I)
      PPE1(I)=PE1(I)
23 CONTINUE
      DO 1 I=1,N
      A(I,1,1)=COS(THA(I))
      A(I,1,2)=-SIN(THA(I))*COS(ALP(I))
      A(I,1,3)=SIN(THA(I))*SIN(ALP(I))
      A(I,1,4)=AA(I)*COS(THA(I))
      A(I,2,1)=SIN(THA(I))

```

```

A(I,2,2)=COS(THA(I))*COS(ALP(I))
A(I,2,3)=-COS(THA(I))*SIN(ALP(I))
A(I,2,4)=AA(I)*SIN(THA(I))
A(I,3,1)=0.0
A(I,3,2)=SIN(ALP(I))
A(I,3,3)=COS(ALP(I))
A(I,3,4)=S(I)
A(I,4,1)=0.0
A(I,4,2)=0.0
A(I,4,3)=0.0
A(I,4,4)=1.0
1 CONTINUE
DO 2 I=1,4
DO 2 J=1,4
AD1(I,J)=A(1,I,J)
AD2(I,J)=A(2,I,J)
AD3(I,J)=A(3,I,J)
AD4(I,J)=A(4,I,J)
AD5(I,J)=A(5,I,J)
AD6(I,J)=A(6,I,J)
2 CONTINUE
CALL MATMLT(A,AD1,B,4,4,4)
CALL MATMLT(B,AD2,C,4,4,4)
CALL MATMLT(C,AD3,D,4,4,4)
CALL MATMLT(D,AD4,E,4,4,4)
CALL MATMLT(E,AD5,F,4,4,4)
DO 63 I=1,3
RJ2(I)=AD1(I,4)
DV2(I)=AD1(I,3)
RJ3(I)=B(I,4)
DV3(I)=B(I,3)
RJ4(I)=C(I,4)
DV4(I)=C(I,3)
RJ5(I)=D(I,4)
DV5(I)=D(I,3)
RJ6(I)=E(I,4)
DV6(I)=E(I,3)
63 CONTINUE
CALL VECVEC(RJ2,DV2,CON1,3)
CALL VECVEC(DV2,DV2,CON2,3)
CON3=CON1/CON2
CALL SCAVEC(CON3,DV2,VL2,3)
CALL VEC SUB(RJ2,VL2,PE2,3)
C
C ..... BY NOW PE2 AND DV2 THE R2 AND N2 RESPECTIVLY ARE KNOWN ...
C
CALL VECVEC(RJ3,DV3,COM1,3)
CALL VECVEC(DV3,DV3,COM2,3)
COM3=COM1/COM2
CALL SCAVEC(COM3,DV3,VL3,3)
CALL VEC SUB(RJ3,VL3,PE3,3)
C
C ..... BY NOW R3 AND N3 ARE KNOWN
C
CALL VECVEC(RJ4,DV4,COP1,3)
CALL VECVEC(DV4,DV4,COP2,3)
COP3=COP1/COP2
CALL SCAVEC(COP3,DV4,VL4,3)
CALL VEC SUB(RJ4,VL4,PE4,3)
C

```

```

C
CALL VECVEC(RJ5,DV5,COR1,3)
CALL VECVEC(DV5,DV5,COR2,3)
COR3=COR1/COR2
CALL SCAVEC(COR3,DV5,VL5,3)
CALL VECSUB(RJ5,VL5,PE5,3)

C
C
CALL VECVEC(RJ6,DV6,COQ1,3)
CALL VECVEC(DV6,DV6,COQ2,3)
COQ3=COQ1/COQ2
CALL SCAVEC(COQ3,DV6,VL6,3)
CALL VECSUB(RJ6,VL6,PE6,3)
RETURN
END

C ..... SUBROUTINES .....
C
C ..... T(M,P)=A(M,N)*U(N,P) .....

SUBROUTINE MATMLT(A,U,T,M,N,P)
INTEGER P
DIMENSION A(4,4),T(4,4),U(4,4),X(4),Z(4),X1(3),Y1(3),Z1(3)
DO 1 I=1,M
DO 1 J=1,P
1 T(I,J)=0.0
DO 2 I=1,M
DO 2 J=1,P
DO 2 K=1,N
2 T(I,J)=A(I,K)*U(K,J)+T(I,J)
RETURN

C
ENTRY MATVEC(A,X,Z,M,N)
DO 5 I=1,M
5 Z(I)=0.0
DO 6 I=1,M
DO 6 J=1,N
6 Z(I)=A(I,J)*X(J)+Z(I)
RETURN

C
ENTRY VECSUB(X1,Y1,Z1,N)
DO 4 I=1,N
4 Z1(I)=X1(I)-Y1(I)
RETURN

C
ENTRY VECVEC(X1,Y1,S,N)
S=0.0
DO 9 I= 1,N
9 S=S+X1(I)*Y1(I)
RETURN

C
ENTRY SCAVEC(S,X1,Y1,N)
DO 7 I=1,N
7 Y1(I)=S*X1(I)
RETURN

C
ENTRY VECSUM(X1,Y1,Z1,N)
DO 8 I=1,N
8 Z1(I)=X1(I)+Y1(I)
RETURN

C

```

```
ENTRY VECRS(X1,Y1,Z1)
Z1(1)=X1(2)*Y1(3)-Y1(2)*X1(3)
Z1(2)=X1(3)*Y1(1)-X1(1)*Y1(3)
Z1(3)=X1(1)*Y1(2)-Y1(1)*X1(2)
RETURN
```

C

```
ENTRY VECLN(X1,S,N)
SUMSQX=0.0
DO 12 I=1,N
12 SUMSQX=SUMSQX+X1(I)*X1(I)
S=(SUMSQX)**.5
RETURN
END
```

VITA⁽¹⁾

Alireza Behboud

Candidate for the Degree of

Master of Science

Thesis: WORKSPACE AND JOINT DISPLACEMENT COMPARISON OF 3R and 4R
ROBOTS

Major Field: Mechanical Engineering

Biographical:

Personal Data: Born in Teheran, Iran, October 7, 1957, the son
of Mr. and Mrs. Javad Behboud.

Education: Graduated from Alborz High School, Teheran, Iran,
in 1975; received Bachelor of Science in Mechanical Engin-
eering degree from Oklahoma State University in July 1980;
completed the requirements for the Master of Science degree
at Oklahoma State University in July, 1982.

Professional Experience: Graduate Teaching Assistant, School of
Mechanical and Aerospace Engineering, Oklahoma State Uni-
versity, August 1980 - May 1982.